1999

An improved binary feedback flow control scheme for ATM networks

Li Xue
University of Wollongong

AN IMPROVED BINARY FEEDBACK FLOW CONTROL SCHEME FOR ATM NETWORKS

A thesis submitted in fulfillment of the requirements for the award of the degree

HONORS MASTER OF ENGINEERING

from

UNIVERSITY OF WOLLONGONG

by

LI XUE, B. ENG., M. ENG.

SCHOOL OF ELECTRICAL, COMPUTER AND TELECOMMUNICATION ENGINEERING

1999

Abstract

This thesis is concerned with the design and analysis of a high performance binary feedback flow control scheme primarily targeted at Available Bit Rate (ABR) services in Asynchronous Transfer Mode (ATM) networks. Eventhough the focus is on ATM based ABR services the proposed binary feedback scheme and analytical approach is generic in nature and can be applied to other networks. A simple network model is considered where a common bottleneck distant queue is shared by a number of different round-trip delay source-destination pairs. The Mitra-Seery (MS) algorithm (Bonomi, Mitra and Seery, 1995) is used as a basis for adapting the source transmission rate.

The approach taken was firstly to model the binary feedback MS algorithm system in the frequency domain. This is in contrast with existing literature where a time domain approach is used. A frequency domain method overcomes the major difficulty associated with time domain approaches in that it simplifies greatly the analysis of multiple Virtual Connections (VC). The binary feedback scheme is modelled as a system of delay differential equations where the distant queue is linearised by assuming that it is under heavy load conditions.

The thesis then applies (for the first time) Describing Function (DF) analysis to the binary feedback scheme to establish the nature of limit cycle behaviour (i.e., sustained oscillations of the source transmission rate) and system stability. This approach provides us with the necessary tools for approximately determining the amplitude and frequency of limit cycle behaviour. More importantly it provides the required theoretical insight which will enable binary feedback system designers to avoid limit

cycle behaviour. Note that limit cycle behaviour remains as one of the most detrimental and well documented problems associated with binary feedback schemes in the sense that such networks are generally characterised by sustained transient behaviour resulting in the need for larger queues within the network switches. The accuracy and validity of the describing function method is analysed and confirmed using simulation. For the case of multiple greedy sources our results indicate that the oscillation characteristics are dependent on the average round trip delay of all sources. For example, when the average delay increases the amplitude of oscillation also increases.

A modified MS (MMS) algorithm is proposed which results in oscillation free behaviour. It turns out that the optimal choice of parameters also depends on the number of active connections. We also show how the queue lengths can be further minimised by appropriate choice of the gain parameters associated with rate decrease factor. Extensive simulation results are provided to establish the performance of the proposed MMS algorithm in a variety of network conditions. For instance, we firstly considered the case where all sources are greedy and all of the bandwidth is available for ABR services. Secondly, we examined the case where the sources are bursty and further where other traffic is present such as that generated by constant bit rate (CBR) and variable bit rate (VBR) services. The overall results clearly indicate that the proposed MMS algorithm does indeed perform significantly better that the MS algorithm.

Acknowledgment

I would like to express my thanks to my supervisor Professor Chicharo for offering his time, patience and expertise throughout this thesis work.

List of Symbols

a_i, b_i	Fourier coefficients
A, A_i, A^+, A^-, $A_i(t)$, $A^+(t)$	gain parameters
Γ, Γ_i, Γ^-, Γ^+	damping parameters
C	bias
D, D_1, $D_{\Sigma J}$, $D_{\Sigma J+1}$	amplitudes of limit cycles
$\phi(t)$, $\phi_i(t)$, $\Phi(s)$	allowed cell rates
$\phi_s(t)$	real cell transmission rate
Φ_Σ	stationary rate of buffer input
$G(s)$, $G_1(s)$, $G_2(s)$, $G_3(s)$	transfer functions
J	the number of active virtual connections
k	parameter for setting a target bandwidth
$u(t)$, $u_i(t)$, $U(s)$	binary feedback functions
$m(t)$	binary feedback function for implementing use-it-or-lose-it policy
μ	queue service rate
N_1	nonlinear element or its describing function
λ_1, λ_2	intensity parameters of Poisson distributions
$q(t)$, $q_s(t)$	queue length
q_T	buffer threshold
s	complex variable of Laplace transform
t	time in seconds
τ, τ_i	round-trip propagation time delays in seconds
ν, ν_i	minimum rates associated with virtual connections

ω, ω_1, $\omega_{\Sigma J}$	frequencies of limit cycles
$x(t)$	input rate of nonlinear element
X_1, X_2	amplitudes of harmonics
$y(t)$	rate of bursty source
$z(t)$	output rate of nonlinear element

List of Acronyms

ABR	Available Bit Rate
ACR	Allowed Cell Rate
ATM	Asynchronous Transfer Mode
BECN	Backward Explicit Congestion Notification
BN	BECN (bit in RM cell)
CAC	Connection Admission Control
CAPC	Congestion Avoidance with Proportional Control
CBR	Constant Bit Rate
CCR	Current Cell Rate
CDF	Cutoff Decrease Factor
CI	Congestion Indication (bit in RM cell)
DF	Describing Function
DIR	Direction (bit in RM cell)
EFCI	Explicit Forward Congestion Indication
EPRCA	Enhanced Proportional Rate Control Algorithm
ER	Explicit Rate
ERICA	Explicit Rate Indication for Congestion Avoidance
ERF	Minimum Decrease Required
ERU	Maximum Increase Allowed
FIFO	First In First Out queue service discipline
ICR	Initial Cell Rate
LAN	Local Area Network
MACR	Mean Allowed Cell Rate
M_{rm}	Minimum number of cells between RM cells generation
MCR	Minimum Cell Rate
NI	No Increase (bit in RM cell)

N_{rm}	Maximum number of cells between RM cell generation
OSU	Ohio State University
PCR	Peak Cell Rate
PRCA	Proportional Rate Control Algorithm
RDF	Rate Decrease Factor
RIF	Rate Increase Factor
RM	Resource Management
UBR	Unspecified Bit Rate
UPC	Usage Parameter Control
VBR	Variable Bit Rate
VPC	Virtual Path Connection

Contents

Chapter 1

Preliminaries

1.1 Introduction

Asynchronous Transfer Mode (ATM) is a networking protocol, which has the potential to support applications with specified tolerances for delay, jitter, and cell loss. Different traffic classes have been defined by the ATM Forum (1996) to address the service requirements including Constant Bit Rate (CBR), real-time Variable Bit Rate (rt-VBR), non-real-time Variable Bit Rate (nrt-VBR), Unspecified Bit Rate (UBR) and Available Bit Rate (ABR). CBR and rt-VBR provide cell loss and delay guarantees and can be used for real-time applications, like circuit emulation, voice and entertainment-quality video. Nrt-VBR provides cell loss guarantees only which means that it is suitable for those applications that expect a low cell loss ratio. The UBR and ABR have been designed for data applications, such as file transfer and email. UBR does not specify any performance guarantees. ABR provides minimum cell rate guarantees and attempts to minimise the cell transfer delay and cell loss ratio as much as possible.

Among the five traffic classes CBR and VBR are assigned a higher priority by the network while ABR and UBR services can use the remaining bandwidth. Note also that ABR has priority over UBR. Figure 1.1 depicts typical link capacity allocation among the various traffic classes. Clearly ABR and UBR are designed to take advantage of any excess capacity thus maximising link utilization. ATM allows all of these services to be supported efficiently in a single network via appropriate traffic management mechanisms.

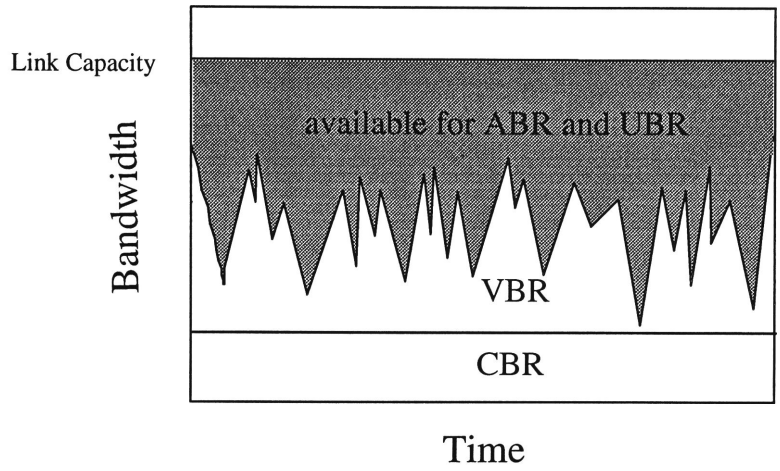

Figure 1.1 *ATM traffic classes link capacity allocation.*

Traffic management endeavors to provide specified quality of services for various traffic classes while maintaining high utilization (Jain, 1996). A central problem is the issue of congestion, which occurs whenever traffic from user nodes exceeds the capacity of the network. There are two sets of mechanisms to handle congestion: traffic and congestion control (Stallings, 1997). The first is for congestion avoidance; the second is for the minimisation of congestion intensity, spread, and duration. The available traffic and congestion control mechanisms are summarised as the following (ATM Forum, 1996):

(i) Connection Admission Control (CAC)

The network accepts new connections only if sufficient resources are available.

(ii) Usage Parameter Control (UPC)

UPC is used to monitor existing connections to detect any violation of connection set up agreements and take appropriate action.

(iii) Selective Cell Discarding or Frame Discarding

A congested network element may either selectively discard cells, which have lower priority or belong to a non-compliant connection, or discard frames to avoid congestion collapse.

(iv) Traffic Shaping

Traffic Shaping is used to smooth out traffic flow at the ingress point.

(v) Explicit Forward Congestion Indication (EFCI)

Any congested node may set the EFCI bit in the cell header to inform the destination that there is congestion. The destination may in turn inform the sources, which should take appropriate action, namely, reduce its transmission rate.

(vi) Resource Management using Virtual Paths

A virtual path (VP) connection provides a convenient means of grouping similar virtual connections (VCs). Network resources can be allocated simply and efficiently using VPs.

(vii) ABR Flow Control

ABR flow control is designed to enable the network to allocate the available bandwidth fairly and efficiently among ABR sources using feedback. It allows the sources to limit their data transmission to rates allowed by the network. As we explain later, ABR flow control can be implemented in various ways.

For various traffic classes ATM networks can implement one or a combination of above mechanisms in order to ensure the desired quality

of service for various users. In this thesis, we address the problem of analysis and design of ABR flow control.

ABR flow control is a technique where a source adapts its cell transmission rate by using feedback information from the network. Credit-based and rate-based schemes were two leading techniques for implementing this closed-loop control (Yang and Reddy, 1995, Chen, Liu and Samalam, 1996, Jain, 1996). The credit-based scheme employs a link-by-link virtual circuit flow control technique (Kung, Blackwell and Chapman, 1994) where each connection must obtain buffer reservations for its cell transmission for each link. This reservation is given in the form of a credit balance, whereby a node cannot send any cell to the next node until it gains credits from it. The credit-based scheme minimises the transmission delay by controlling buffer allocation directly, which guarantees also that no cell is lost due to buffer overflow (Kung and Morris, 1995). However, the credit-based scheme requires separate virtual queues for each connection and results in considerable hardware complexity (Siu and Tzeng, 1995, Chen, Liu and Samalam, 1996). As a result the ATM Forum voted for rate-based flow control in 1994. The rate-based scheme is also a closed-loop control technique. However, the feedback information is utilised to change the rate at which each source is submitting cells into the network in response to changing network conditions (Bonomi and Fendick, 1995). According to network environment, the rate-based scheme encompasses a broad range of implementations associated with different levels of complexity to meet various performance requirements and cost budgets. It allows flexibility in vendor implementation to tailor products to suit particular market requirements (Krishnan, 1997).

The next section briefly explains the various rate-based flow control schemes for ABR service in ATM networks. Section 1.3 states the underlying problems claimed with the thesis. Finally, Section 1.4 provides a brief outline of the contributions.

1.2 Rate-based flow control for ABR in ATM

The rate-based flow control scheme allows sources to adapt their transmission rates according to network conditions. The network information is sent to the sources as feedback via resource management (RM) cells. The format of the RM cells is shown in Table 1.1.

***Table 1.1** Fields in RM cell (ATM Forum, 1996)*

ATM Header		5 bytes
Protocol Identifier	(ID)	1 byte
Direction	(DIR)	1 bit
Backward Explicit Congestion Notification	(BN)	1 bit
Congestion Indication	(CI)	1 bit
No Increase	(NI)	1 bit
Request/Acknowledge	(RA)	1 bit
Explicit Rate	(ER)	2 bytes
Current Cell Rate	(CCR)	2 bytes
Minimum Cell Rate	(MCR)	2 bytes
Queue Length	(QL)	4 bytes
Sequence Number	(SN)	4 bytes
Reserved		30 bytes
Reserved + CRC 10		2 bytes

An RM cell has the standard ATM header. The direction (DIR) field indicates the direction of the RM cell. The BN bit is set only when switch or destination generate a backward explicit congestion notification (BECN). The CI bit is set whenever congestion occur. The NI bit is used to avoid the source increasing its rate when a switch senses impending congestion. The explicit rate (ER) field is used to indicate the transmission rate allowed to the source. The current cell rate field is used

by the source to indicate its current rate. The MCR field is set to the minimum rate required by the source.

The CI, NI, BN and ER fields are used by the network to give feedback to the sources. Depending on the fields used various nodes support rate-based schemes can be classified into two categories including: binary feedback and explicit rate feedback.

1.2.1 Binary feedback

A binary feedback mechanism uses only a single bit in an RM cell for feedback, which indicates if a switch is congested, or not. Accordingly the sources will then increase or decrease their rates by a pre-determined amount. A number of schemes have been proposed for binary feedback control, these are discussed next.

1.2.1.1 Newman's scheme

The first rate-based scheme was proposed by Newman (1994) for ABR services in ATM local area networks (LAN). In this scheme, a congested switch periodically sends a backward explicit congestion notification (BECN) via an RM cell to each active source. The source reduces its rate exponentially whenever a BECN cell is received. Otherwise the source continues to increase its rate until it reaches the peak cell rate.

Because the control cells are sent directly from a congested node to the source, this scheme has a fast response time. However, if the control cells are lost due to heavy congestion in the feedback path, the source will keep increasing its rate and will eventually aggravate the congestion. This problem was fixed by using positive feedback; that is, a source

decreases its rate by a default value while no RM cells are received. It may increase its rate only if a RM cell is received indicating that there is no congestion.

1.2.1.2 Hluchyj-Yin scheme

The scheme proposed by Hluchyj and Yin (1994) uses an end-to-end flow control approach based on queue length of a switch. When a queue threshold is exceeded it sets the EFCI bit in the header of forward data cells. The destination monitors the EFCI bit at fixed intervals and sends an RM cell back to the source when *EFCI=0*. No RM cell will be sent back when *EFCI=1*. The source increases its rate if a RM cell is received and decreases its rate while no RM cell is received.

The algorithm used for adapting transmission rate in the Hluchyj-Yin scheme can be classified as a linear-increase/exponential-decrease algorithm. This type of algorithms was shown to be sensitive to control parameters and feedback delay (Mukherjee and Strikwerda, 1991).

1.2.1.3 Proportional rate control algorithm (PRCA)

In PRCA (Barnhart, 1994) the RM cells are generated at a rate roughly proportional to the source rate. This is an important change in comparison with the Hluchyj-Yin scheme (1994). The sources set the EFCI on every cell except the N_{rm}^{th} cell. The destination monitors every cell received, and sends a RM cell back to the source if there is any cell with an *EFCI=0*. The sources will continually decrease their rates exponentially until they receive an RM cell, after which they will increase their rates by a fixed increment. The overall rate increase is approximately exponential.

A weakness of PRCA is that it may suffer from unfairness problems in certain situations when all connections share a common first-in-first-out (FIFO) buffer. A connection travelling more nodes has a higher probability of having EFCI set than those travelling a relatively smaller number of nodes. Thus, the connection, which travels more nodes, gets fewer chances to increase its rate. This is referred to as the "beat-down" problem (Bennett and Jardins, 1994).

In order to overcome this unfairness a fair share is computed at a switch in the selective feedback (Ramakrishnan, Chiu and Jain, 1987) and intelligent marking (Barnhart, 1994) schemes. If congestion occurs the switch sets the EFCI bits in cells belonging to only those VCs whose rates are above the fair share. Those VCs whose rates are below the fair share are not affected. Further, based on simulation studies Kolarov and Ramamurthy (1996) determined that unfairness could be alleviated by giving priority to network transit traffic over local traffic at each node.

1.2.1.4 Mitra-Seery (MS) algorithm

MS algorithm is an exponential-increase/exponential-decrease algorithm initially proposed by Mitra and Seery (1993). It was recently examined by Bonomi, Mitra and Seery (1995) in order to improve its stability and fairness. This algorithm is suitable for bipolar feedback mechanism, that is, RM cells are sent for both increasing and decreasing the source rate. The RM cells may be sent either at fixed intervals or for every N_{rm} data cells. Two key parameters are introduced "gain" for response and "damping" for stability. If both parameters are selected properly stability and fairness can be achieved.

1.2.1.5 EFCI scheme with early congestion detection (EFCI-ECD)

Zhao, Li and Sigarto (1996) pointed out that congestion detection using queue length threshold has the disadvantage of delayed congestion detection where no congestion is detected unless the queue is above the threshold. They proposed an early congestion detection mechanism whereby a bandwidth threshold instead of queue length threshold is used. Their EFCI-ECD scheme is based on the condition that congestion is mainly caused by low frequency traffic variations, which can be estimated by filtering the input rate of a buffer (Li and Hwang, 1993). The congestion is then detected whenever the filtered traffic rate exceeds a pre-assigned link bandwidth threshold.

1.2.2 Explicit rate feedback

Explicit rate (ER) feedback switches determine the fair share of the bandwidth for each connection and explicitly specify the rate to be used by the source (Charny, Clark and Jain, 1995). One of the key issues of the ER feedback schemes is how to compute the fair share at switches. We will briefly review several switch algorithms and describe the current framework for ABR flow control in ATM Forum.

1.2.2.1 Enhanced proportional rate control algorithm (EPRCA)

EPRCA (Roberts, 1994, Roberts *et al.*, 1994) combines the PRCA with ER feedback. It can interoperate with both binary and ER feedback switches on a communication path. The source generates one RM cell for every N_{rm} data cells with *EFCI=0* in the forward direction. On connection establishment the sources initialise the ER field to their peak

cell rate (PCR) and set the congestion bit (CI) to zero. This specific use of RM cells depends on the type of intermediate switches.

If an intermediate switch does not support explicit rate feedback, it ignores the content of the RM cell and sets the EFCI bit in the headers of all data cells to *1* when congestion occurs. The destination filters the EFCI bit set by the switch. When the next RM cell arrives, the destination sets CI bit in the RM cell to *1* and returns it to the source if the last seen data cell has *EFCI=1*. Otherwise, the RM cell is sent back with *CI=0*.

When an intermediate switch is an ER switch it computes a mean allowed cell rate (MACR) and a fair share for all virtual connections (VCs) as follows.

$$\begin{aligned} MACR &= (1-\alpha)\,MACR + \alpha * CCR \\ fairshare &= DPF * MACR \end{aligned} \tag{1.1}$$

where CCR is the current cell rate, α is an exponential averaging factor and DPF is the down pressure factor. The suggested values of α and DPF are *1/16 and 7/8,* respectively. The switch reduces the ER field in the returning RM cells to the fair share if the value in the ER field is higher. Otherwise, no adjustment is made. The switch can also set *CI=1* in the returning RM cells if its queue length exceeds a predetermined threshold.

Sources always decrease their ACR exponentially except when the RM cell is received. For *CI=0* ACR is determined using

$$ACR = Min(ACR + AIR,\ ER,\ PCR) \tag{1.2}$$

where AIR is the additive increase rate. If *CI=1*, the ACR remains unchanged.

EPRCA is flexible because both binary feedback and ER feedback switches are allowed to co-exist in the same VC. Its main problem is the unfairness that may occur when the mean ACR is not a good estimate of the fair share (Chiussi, Xia and Kumar, 1996).

1.2.2.2 Congestion avoidance scheme

This scheme was proposed by Jain, Kalyanaraman and Viswanathan (1994). It is also known as the Ohio State University (OSU) scheme. In this approach the change in queue length is monitored for congestion detecting. The source sends the RM cells at a fixed time interval. At the switch a current load factor is computed as follows:

$$z = \textit{input rate} / \textit{target rate} \tag{1.3}$$

where the input rate is measured by counting the number of cells received by the switch during a fixed averaging interval and the target rate is set to the value that is close to the link rate. All sources are expected to divide their rate by the load factor z. However, if z is close to *1* for a small difference Δ, the fair share is determined by

$$\textit{Fair share} = \textit{target rate} / \textit{number of active sources} \tag{1.4}$$

A source is expected to divide its rate by $z/(1-\Delta)$ if the rate is below the fair share. The source divides its rate by $z/(1+\Delta)$ if the rate is higher than the fair share.

1.2.2.3 Explicit rate indication for congestion avoidance (ERICA)

ERICA scheme was proposed by Jain, Kalyanaraman and Viswanathan (1995). In this scheme, the source generates RM cells after every N_{rm} data cells. The switches calculate the fair share and the load factor z in the same way as the OSU scheme. However, the ER values are computed using

$$\begin{aligned} &ER\ based\ on\ load = ER_1 = CCR / z \\ &ER\ based\ on\ load\ and\ fair\ share = ER_2 = Max(fair\ share, ER_1) \end{aligned} \tag{1.5}$$

The switch finally obtains ER_3 value after comparing ER_2 with ER in the RM cell as follows:

$$ER_3 = Min(ER\ in\ the\ RM\ cell,\ ER_2) \tag{1.6}$$

A feature of ERICA is that the switches that implement ERICA only require two parameters, that is, the target utilisation for determining target rate and the fixed averaging interval for measuring the input rate.

1.2.2.4 Congestion avoidance using proportional control (CAPC)

The fair share calculation in the CAPC scheme (Barnhart, 1994) is different from that in the OSU scheme and the ERICA. In the case where $z < 1$

$$fair\ share = fair\ share * Min(ERU, 1 + (1-z) * Rup) \tag{1.7}$$

where Rup is a rate increase factor and ERU is the maximum increase allowed, which is set to *1.5*. If $z > 1$

$$fair\ share = fair\ share * Max(ERF, 1 - (1-z) * Rdn) \tag{1.8}$$

where Rdn is a rate decrease factor and ERF is the minimum decrease required and is set to *0.5*. The fair share is the maximum rate allowed by the switch for the VCs to use.

CAPC is oscillation-free in steady state and simple to implement where ER is determined based on the bandwidth demand estimation algorithm (ATM Forum, 1996)

1.2.2.4 Current specification in ATM Forum

The current specification is largely based on the ideas of EPRCA with some differences in details (ATM Forum, 1996). The main differences are:

(i) The source will continue to send RM cells after every N_{rm}-1 data cells are transmitted or after at least M_{rm} data cells are transmitted and at least T_{rm} time has elapsed.

(ii) The data cells are sent at a rate less than or equal to ACR.

(iii) The source adapts its rate using the information carried by backward RM cells. If the congestion bit *CI=1*, then the source reduces its rate using

$$MCR \leq ACR \leq Min(ACR - ACR * RDF, ER) \tag{1.9}$$

where RDF is the rate decrease factor and MCR is the minimum cell rate. If *CI=0* and the no increase bit *NI=0*, the source will increase its rate to

$$ACR \leq Min(ACR + RIF * PCR, ER, PCR) \tag{1.10}$$

where RIF is the rate increase factor.

(iv) A mechanism has been added to back off the source rate when a source starts transmitting after being idle or congestion causes the loss of backward RM cells. If the time interval between forward RM cells is greater than the ACR the decrease time factor (ADTF) ACR shall be reduced to ICR (initial cell rate).

If the source has sent C_{rm} forward RM cells without receiving a backward RM cell the source reduces the ACR to

$$MCR \leq ACR \leq Min(ACR - ACR * CDF, ER) \qquad (1.11)$$

where CDF is the cutoff decrease factor.

(v) The destination turns all RM cells received back to the source and changes the direction bit from "forward" to "backward".

(vi) The destination (having internal congestion) may reduce ER to whatever rate it can support and/or set *CI=1* or *NI=1*.

(vii) A congested switch may generate a backward RM cell, resulting in a fast response time. The *CI, NI* and *BN* bits in the backward RM cell are set to *1*.

(viii) The source and switch may implement a use-it-or-lose-it policy to reduce their ACR to a value which approximates the actual cell transmission rate.

(ix) The current specification does not mandate any particular switch algorithm and manufacturers are free to use their own approach if they wish. Naturally, some of the possible algorithms include: EPRCA, congestion avoidance schemes, ERICA and CAPC.

These are all included in the Informative Appendix I (ATM Forum, 1996) as possible switch schemes.

1.2.3 Advantages and disadvantages of the various approaches

1.2.3.1 Binary feedback schemes

Binary feedback schemes have the following attractive features for ABR flow control:

(i) Simple to implement

Simplicity is one of the basic advantages of the binary feedback control scheme. Only a single bit in the header of forward data cells is required and the switches detect congestion by simply monitoring their queue length (excluding the EFCI-ECD scheme). In addition only a single bit is used to inform the congestion. Scalable in the sense that as the number of VCs increases at each switch no further work is required by the switch.

(ii) Low cost

Binary feedback switches are less complex than ER switches because ER switches need to measure cell rates and calculate the explicit rate for sources.

The disadvantages are:

(i) Oscillation

The binary feedback indication only tells the source whether it should go up or down and the source must determine how much higher or lower. As a result the rate will oscillate around the congestion point. Larger buffers are required to avoid cell loss (Siu and Tzeng, 1995,

Charny, Clark and Jain, 1995). Consequently, longer delay will be introduced.

(ii) Unfairness.

When all the connections share a common buffer some connections may have an unfair share of the bandwidth. One example is the "beat down" problem associated with the PRCA mechanism. Complexity at switches may increase in order to solve this problem.

In summary, the binary feedback schemes are simple and cost effective however, a lot of work remains to be done in order to improve their performance.

1.2.3.2 Explicit rate schemes

The ER feedback schemes use more information about the network and, hence, result in the following attractive features (Charney, Clark and Jain, 1995, Jain, 1996):

(i) Straight-forward policing

The explicit rate in the returning RM cells can be used directly by a policing algorithm.

(ii) Fast convergence time

The system comes to the optimal operating point after several round-trip times.

(iii) Robust against loss of RM cells

Next correct RM cell will bring the system to the correct operating point.

ER feedback schemes have following disadvantages:

(i) High implementation complexity

The switch algorithms are complex. For calculating the explicit rate, the ABR demand is measured, such as those for OSU, ERICA and CAPC, or estimated, such as the algorithm for EPRCA. In other words, switches have to a lot more work in determining the explicit rate for each ABR connection.

(ii) Difficult to select parameters

The ER schemes use a number of parameters whose values are pre-determined. For example, DPF and α in the EPRCA; Rup, Rdn, ERU and ERF in the CAPC; the length of the time interval for measuring the input rate in the OSU and ERICA. Some of parameters are difficult to choose because of a tradeoff between steady state performance and transient state performance. Any incorrect parameter selection will produce incorrect ER computation, which may lead to unfairness, large queue sizes and associated performance degradation (Krishnan, 1997, Chiussi, Xia and Kumar, 1996, Afek, Mansour and Ostfeld, 1996).

1.3 Problem statement and research objectives

This thesis studies a binary feedback flow control scheme for ABR service in ATM networks. Our objective is to significantly improve its performance such that its low implementation complexity can be capitalised.

Sustained oscillation is one of the main problems of binary feedback flow control schemes. The resulting oscillation not only introduces delay in

the bottleneck node but also requires large amounts of buffer resources. Oscillating ABR traffic also leads to concerns about its impact on other non-ABR traffic within the public networks (Zhao, Li and Sigarto, 1996). Hence the specific goals of this thesis are to investigate the nature of oscillations and secondly to develop mechanisms which will eliminate or reduce significantly such oscillations. The following tasks will be carried out:

(i) A Laplace domain model will be developed for the binary feedback system.

(ii) Apply describing function analysis to establish the stability and limit cycle behaviour of the system.

(iii) Using results from describing function analysis we will design an oscillation-free binary feedback algorithm.

(iv) Carry out an extensive performance evaluation under bursty sources and background traffic.

A control system engineering approach will be applied for the analysis and design of oscillation free operation. Close examination of the feedback mechanism studied by Bonomi, Mitra and Seery (1995) indicates that it is similar to a traditional relay-based servo control system (West, 1960, Gelb and Velde, 1968, Atherton, 1981). However, the ABR flow control problem is dynamically much more complex than the servo control problem. The main difficulties includes:

(a) Non-linear queue characteristics have to be accounted for.

(b) The ATM network involves multiple VCs, each has its own propagation time delay. Further, the associate time delays are stochastic in nature.

Nevertheless, we believe that the analytical methods which apply to the servo control system can be modified and applied for the analysis and design of the ABR flow control.

1.4 Contribution of the thesis

In this thesis we consider the problem of improving performance of binary feedback flow control for ABR services. The main contribution is achieved by applying nonlinear control theory for the analysis and design of a binary feedback mechanism which is suitable for ABR service in packet networks. The specific contributions include:

(i) A fluid flow model in the Laplace domain is derived for the binary feedback switched network system. The derived models can represent both single VC and multiple VCs network situations.

(ii) Stability and sustained oscillation in the network system is investigated. Quantitative results on the oscillation frequency and amplitude are obtained using the approximate frequency domain technique known as Describing Function (DF) (Gelb and Velde, 1968).

(iii) The accuracy of the DF approach is analysed and established for the application considered.

(iv) A modified MS algorithm (MMS) is proposed to reduce the oscillation caused by the MS algorithm.

(v) The performance of the MMS algorithm is demonstrated and compared with the MS algorithm.

Chapter 2

Network and MS Algorithm Modeling

2.1 Introduction

We consider the network configuration depicted in Figure 2.1, where a number of virtual connections (VCs) feed into a distant switch buffer. The queue service rate, known as the bandwidth of the bottleneck link, is denoted by μ. The switch has a threshold value given by q_T. When the queue length at the switch exceeds this threshold, congestion notification will be set by the switch. It is assumed that the distant switch buffer operates on a First-Come-First-Served (FCFS) basis. The sources are possibly located at different geographical sites. Each VC is assumed to have a different propagation delay. Further, it is assumed (for the sake of simplicity) that the propagation time between a source and the distant switch is equal in both forward and feedback directions.

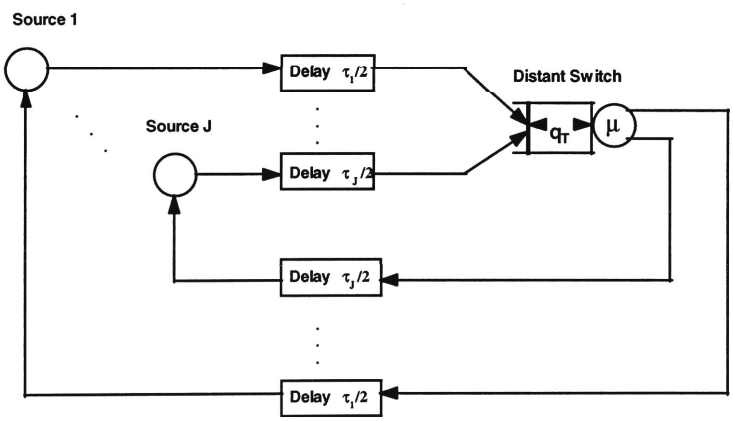

Figure 2.1 *Network model.*

Traffic sources are initially assumed to be "greedy". In other words, a source is assumed to have an infinite amount of data to send and hence will accept whatever capacity it is offered by the network. Greedy sources are particularly, useful in establishing the performance associated with fairness issues (Siu and Tzeng, 1995).

This chapter is organised as follows. Section 2.2 derives models in the Laplace domain for the network and MS algorithm and represents these in block diagram form. Section 2.3 simulates the derived system model using MATLAB SIMULINK toolbox (Math Works Inc, 1996). The derived models are validated by comparing the results with those reported in Bonomi, Mitra and Seery (1995). Section 2.4 concludes this chapter.

2.2 Model of network with MS algorithm in LAPLACE domain

In this section we derive an equivalent Laplace domain model for the network and MS algorithm. The final system block diagram represents the network configuration depicted in Figure 2.1 together with the MS binary feedback algorithm, which is outlined in (Bonomi, Mitra and Seery, 1995). We start from a single VC case, where only one source is active and the source adapts its rate using the MS algorithm. Derivation of the multiple VC model case is carried out in subsection 2.2.2.

2.2.1 Single VC model

A model for the FCFS buffer at a distant switch can be approximately described by a first order differential equation (Bonomi, Mitra and Seery, 1995):

$$\frac{d}{dt}q(t) = \begin{cases} \phi(t-\tau/2) - \mu & if\ q(t) > 0 \\ [\phi(t-\tau/2) - \mu]^{+} & if\ q(t) = 0 \end{cases} \qquad (2.1)$$

where $\phi(t)$ is the flow rate for each source, μ is a constant queue service rate and $q(t)$ is the queue length. $\tau/2$ represents the propagation time between the source and the distant switch buffer. An implicit assumption

of this approach is that the process is viewed as fluid model. This model holds in an environment where the time to transmit a packet is short when compared to the total transfer time, and does not vary significantly from packet to packet (Fendick, Rodrigues and Weiss, 1992). In order to capture the fact that the buffer level is always non-negative the following condition is imposed on Equation (2.1):

$$[x]^+ = \begin{cases} x & if \ x \geq 0 \\ 0 & if \ x < 0 \end{cases} \tag{2.2}$$

The binary feedback from the switch to the source transmitter is defined as:

$$u(t) = sign[q_T - q(t - \tau / 2)] \tag{2.3}$$

where q_T denotes the buffer threshold. The feedback $u(t)=+1$ when the queue length is below the threshold level q_T, while if the queue length is above the set threshold $u(t)=-1$. Note that the feedback information $u(t)$ is either 0 or 1 in practice. The above definition is, however, adopted for convenience of mathematical analysis and does not change the final results. The MS algorithm resides within each VC source and its objective is to determine a suitable flow rate based on the binary feedback information $u(t)$ received from the distant switch buffer. This algorithm was defined by Bonomi, Mitra and Seery (1995) as follows:

$$\frac{d}{dt}\phi(t) = -\Gamma[\phi(t) - v] + Au(t) \tag{2.4}$$

where v is the minimum rate associated with a virtual connection. The parameters Γ and A can be chosen by the MS algorithm designer to achieve the desired performance (Bonomi, Mitra and Seery, 1995).

Assuming zero initial conditions the Laplace transform for Equation (2.4) has the form

$$s\Phi(s) = -\Gamma(\Phi(s) - \frac{\nu}{s}) + AU(s) \tag{2.5}$$

Because the buffer level is always nonnegative the nonlinearity represented in Equation (2.1) can be described in the following way

$$\frac{d}{dt}q(t) = [\phi(t-\tau/2) - \mu][1(\phi(t-\tau/2) - \mu) < OR > 1(q(t))] \tag{2.6}$$

where $<OR>$ denotes the logic OR operation and

$$1(x) = \begin{cases} 1 & if \ \ x > 0 \\ 0 & if \ \ x \leq 0 \end{cases} \tag{2.7}$$

is a step function. The transfer function block diagram for a single VC source using the MS feedback flow control algorithm is depicted in Figure 2.2. It is interesting to note that the system depicted in Figure 2.2 is similar in structure to the classical feedback relay control problem (Ogata, 1990). The feedback signal oscillates between *+1* and *-1* which is equivalent to an amplifier with infinite gain.

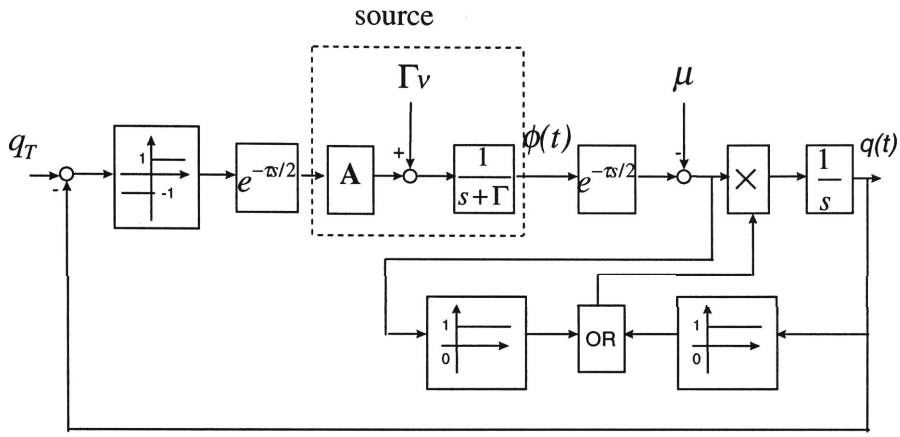

Figure 2.2 *Block diagram of a single VC binary feedback flow control system using the MS algorithm.*

2.2.2 Multiple VC model

We now consider the more realistic situation where there are multiple VCs feeding into a distant switch buffer. The model representing this situation can be derived by modifying Equations (2.1), (2.3) and (2.4) as follows:

$$\frac{d}{dt}\phi_i(t) = -\Gamma_i[\phi_i(t) - \upsilon_i] + A_i u_i(t) \tag{2.8}$$

$$u_i(t) = sign[q_T - q(t - \frac{\tau_i}{2})] \tag{2.9}$$

$$\frac{d}{dt}q(t) = \begin{cases} \sum_{i=1}^{J} \phi_i(t - \tau_i/2) - \mu & if\ q(t) > 0 \\ \left[\sum_{i=1}^{J} \phi_i(t - \tau_i/2) - \mu \right]^+ & if\ q(t) = 0 \end{cases} \tag{2.10}$$

where $i=1, 2, \ldots, J$ and the function $[]^+$ is the same as described in Equation (2.2). The block diagram for the multiple VC case is depicted

in Figure 2.3 where ϕ_i, υ_i and τ_i represent the flow rate, the source minimum rate and the propagation delay for each VC respectively.

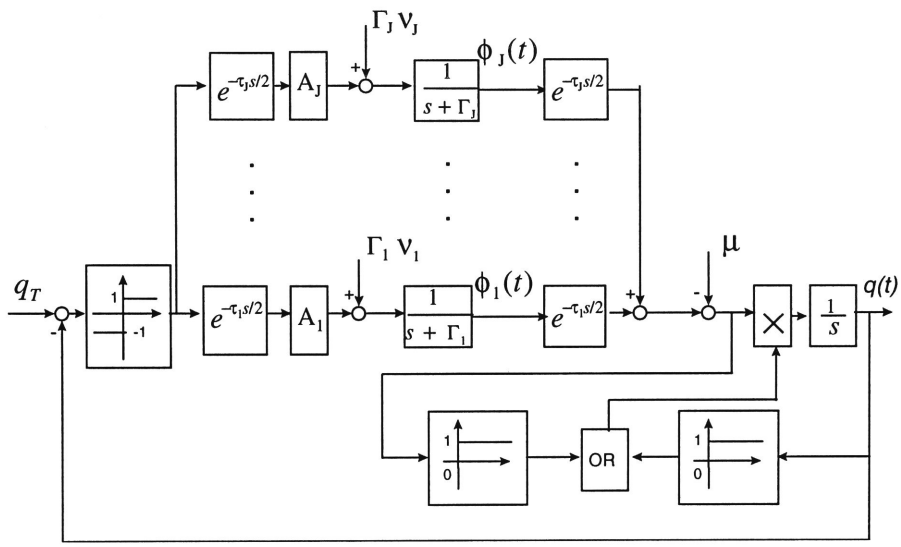

Figure 2.3 *Block diagram of multiple VC binary feedback flow control system.*

2.3 Simulation Results

In this section we implement the single and multiple VC models depicted in Figure 2.2 and Figure 2.3 using the SIMULINK toolbox (Math Works Inc, 1996). The aim is to validate the derived models by comparing the results reported by Bonomi, Mitra and Seery (1995) with those obtained by proposed SIMULINK simulation. SIMULINK is used extensively for modeling and simulating dynamic systems primarily within the control engineering fraternity. It provides a graphical modeling environment based on user-defined block diagrams (that is, transfer functions). Interactions between different parts of a closed-loop system can be visually observed during the process of simulation.

In order to make direct comparisons we use the same parameter values in our simulation as those used in (Bonomi, Mitra and Seery, 1995). Two examples are considered, the first involves a single VC while the second simulation deals with the situation where a VC becomes active and sometime later a second VC comes on line (that is, the multiple VC case). Figure 2.4 depicts the case where a single VC becomes active at time $t=0$, and we consider the effect of various gain (A) values (with a fixed damping factor Γ) in the MS algorithm for the same conditions as reported in Bonomi, Mitra and Seery (refer to Appendix A). The results show that the higher the gain, A, the faster the transient response, however; the amplitude of oscillation also increases.

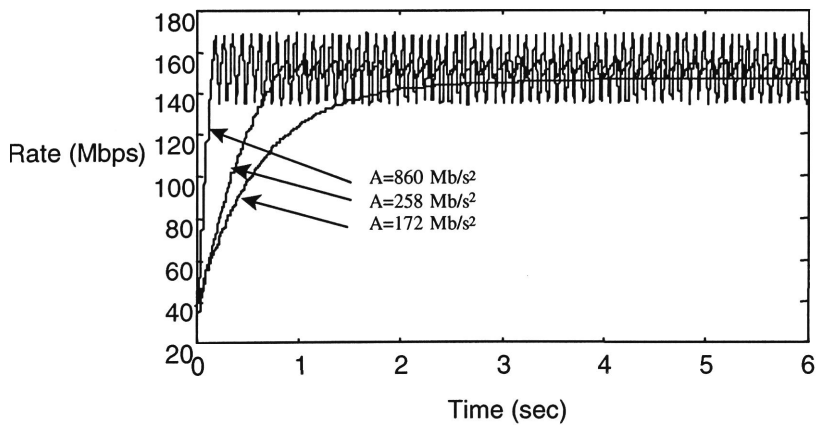

Figure 2.4 *Simulation results of a single VC case. Γ=1.6 1/s, μ=155 Mb/s, υ=34 Mb/s, τ=10 ms, q_T=6.5 cells.*

Table 2.1 makes a comparison between our results and the results obtained by Bonomi, Mitra and Seery (1995) using the PANACEA package (Ramakrishnan and Mitra, 1988). Dynamic characteristics, such as rise time, amplitude and frequency of oscillation, closely match those reported in Bonomi, Mitra and Seery, 1995 (refer to Appendix A). The

results are summarised in Table 2.1 and indicate that the nonlinear model proposed here for a single VC and its subsequent implementation using SIMULINK is an accurate representation.

Table 2.1 *Comparison between the results using PANACEA and SIMULINK.*

Gain A	Frequency of oscillation (Hz)		Amplitude of oscillation (Mb)		rise time (sec)	
(Mb/s^2)	PANACEA	SIMULINK	PANACEA	SIMULINK	PANACEA	SIMULINK
860	12.2	11.8	17.5	17	0.2	0.2
258	6.6	6.7	4.5	4.5	0.8	0.8
172	-	-	-	-	1.1	1.2

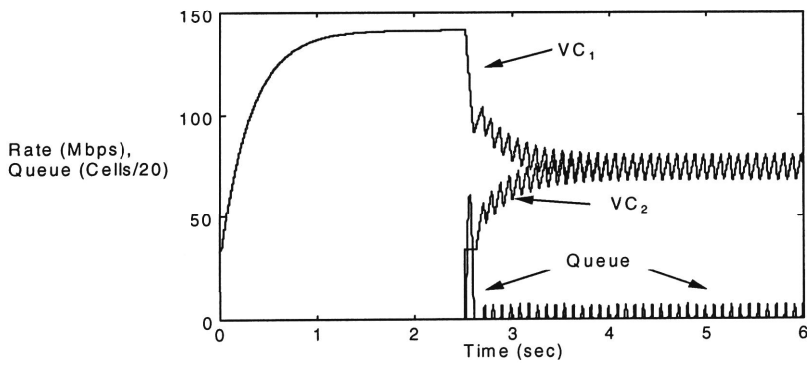

Figure 2.5 *Simulation results of a double VC.* $\Gamma_1=\Gamma_2=3.2$ *1/s,* $\mu=155$ *Mb/s,* $\upsilon_1=\upsilon_2=34$ *Mb/s,* $\tau_1=\tau_2=10$ *ms,* $A_1=A_2=344$ *Mb/s*^{2}*,* $q_T=6.5$ *cells,* VC_1 *turns on at time 0 and* VC_2 *at 2.5 s.*

Figure 2.5 shows the simulation results obtained for the multiple VC case. The aim of this example is to determine the fairshare capability of

the MS algorithm. This is achieved by considering the situation where one VC becomes active at time *t=0* and a second VC is turned on at time *t=2.5* seconds. During steady state, the rates of VC1 and VC2 oscillate between *67 Mb/s* and *81 Mb/s* with the same frequency. Once again there is excellent agreement between these results and those presented in Bonomi, Mitra and Seery, 1995 (refer to Appendix A).

2.4 Conclusion

In this chapter we derived a simple network model together with the MS algorithm using the Laplace domain. A block diagram of the derived models clearly show the feedback structure and its extension from the single VC to the multiple VC case. Simulation results obtained using SIMULINK closely match those reported in (Bonomi, Mitra and Seery, 1995). In the next chapter we will analyse this feedback control system using an analytical nonlinear frequency domain Describing Function method.

Chapter 3

Analysis and Performance Evaluation of the MS Algorithm

3.1 Introduction

The main goal of this chapter is to develop an analytical approach such that one can gain insight into the problem of queue oscillation characteristics associated with binary feedback control. To begin with we first review a number of prior studies in this area. Section 3.2 describes an analytical approach for studying stability and limit cycle behavior. The approach is based on the Describing Function (DF) method, which is effectively a frequency domain technique. Section 3.3 investigates the accuracy of DF approach by harmonic analysis, while Section 3.4 compares simulation results with analytical results in details. Finally, Section 3.5 concludes this chapter.

As discussed in Chapter 1, the binary feedback indication simply tells the source whether it should increase or decrease its rate. As a consequence sustained rate oscillation (limit cycle) often results around the congestion point.

Hluchyj and Yin (1994) derived a model for the analysis of the Hluchyj-Yin scheme and evaluated the maximum queue length of queue oscillation. Yin (1995) also derived a more simplified result for evaluating maximum queue length. The use of a linear-increasing/exponential-decreasing rate in the Hluchyj-Yin (1994) scheme is similar to the algorithm proposed by Jacobson (1988) and Ramakrishnan and Jain (1988). The later is refereed to as the Jacobson, Ramakrishnan and Jain (JRJ) algorithm which is used for window adjustment. Mukherjee and Strikwerda (1991) found that the JRJ algorithm with delay feedback lacks fairness. It was also found that the limit cycle is sensitive to control parameters and feedback delay. Bolot

and Shankar (1990) showed that good steady-state performance could be achieved at the expense of long transient duration.

Analytical models were developed to capture the steady state behaviour of the EPRCA in the network using EFCI switches only (Ramamurthy and Ren, 1995, Ohsaki *et al.*, 1995). It was shown that the EPRCA is equivalent to the PRCA models. Ramamurthy and Ren (1995) evaluated an upper-bound for the maximum queue length and investigated how the values of the various increasing/decreasing parameters affect the system performance. Ohsaki *et al.* (1995) obtained the maximum queue length and established conditions for avoiding under-utilised bandwidth.

Bonomi, Mitra and Seery (1995) evaluated the performance of a network using MS algorithm. Their results indicate that there are two operating regimes for steady state operation. In the unsaturated case the buffers are empty and the feedback system is oscillation free. However, the network bandwidth is not fully utilized. In the saturated case the bandwidth is nearly fully utilized, however, its behaviour is characterised by sustained flow and queue oscillations. Hence the system behaviour is different depending on whether it is in saturated or unsaturated regimes and it will change depending on the number of active VCs. An increase in number of active VCs will result in a higher oscillation amplitude.

All of the above approaches were carried out in time domain using nonlinear differential equations. Because of the complexity in time domain analysis it is very difficult to extend the results to the multiple VC case. Hence, for the case of multiple VCs with different round-trip delays no analytical results are available in literature. Consequently, there are no effective guidelines for system design.

3.2 Limit cycle analysis using the Describing Function method

In this section we study the limit cycle behaviour in the Laplace domain and give an approximate steady state solution using DF Analysis. From a pedagogical point of view it is instructive to review briefly the essence of DF Analysis. In the first instance we introduce the basic concept of the Describing Function method and apply it to the network models obtained in Chapter 2. The limit cycle analysis is carried first of all for a single VC case and is then extended to the multiple VCs model.

3.2.1 Describing Function

The describing function (DF) method (Gelb and Velde, 1968) is often associated with nonlinear control system engineering where it is used for analysis and design of systems with linear and memoryless nonlinear elements. As stated earlier the DF method is an approximate frequency domain approach which can be applied to determine the steady state stability as well as the frequency and amplitude of sustained oscillations (limit cycles) within a nonlinear closed-loop system. From a design point of view the DF method can be used for establishing the parameters of a feedback control system such that limit cycle behaviour can be avoided or minimised.

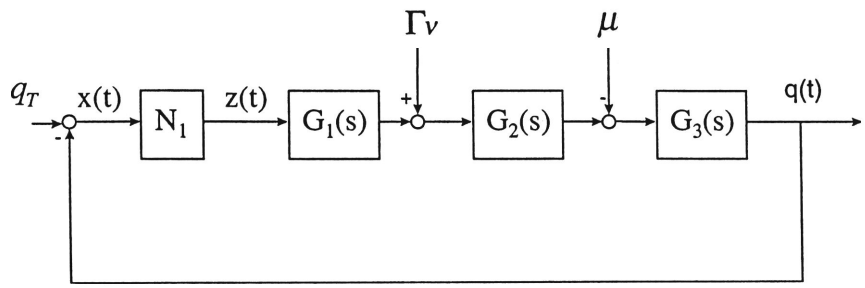

Figure 3.1 *A nonlinear feedback system with sustained oscillation.*

Let us consider the fundamental concepts relating to the DF method. For simplicity we assume that the buffer is either nonempty or its input rate is more than or equal to the buffer service rate μ whenever the buffer is empty. This avoids the apparent impossible case of negative queue length and allows the buffer to be treated as a linear element from a mathematical point of view. Given the above assumption it follows that Equation (2.1) is linear. Moreover, the system described in Figure 2.2 is equivalent to the system shown in Figure 3.1 during steady state operation. Where $G_1(s)= Ae^{-\tau s/2}$, $G_2(s)=\dfrac{e^{-\tau s/2}}{s+\Gamma}$ and $G_3(s)=\dfrac{1}{s}$ are transfer functions which represent the linear parts of the system and N_1 is a static nonlinear element which captures the binary nature of the MS algorithm. In Figure 3.1, $z(t)$ is the feedback information from the switch, and represents the output of the nonlinear element, $x(t)$ is the difference between the threshold q_T and the buffer queue length $q(t)$. Note that the constant queue service rate μ must be nonzero; the buffer threshold q_T and the minimum source rate v may be nonzero. From the feedback control point of view these parameters can be considered external to the closed-loop feedback system and is thus referred to as a forced system. The Describing Function analysis of the forced system assumes that the input

to the nonlinear element is a sinusoid plus a constant bias (Gelb and Velde, 1968). That is:

$$x(t)=C+D\sin\omega t \tag{3.1}$$

Equation (3.1) is known as a dual-input describing function (DIDF). The output *z(t)* can then be expressed as a Fourier series:

$$z(t)=\frac{a_0}{2}+\sum_{n=1}^{\infty}(a_n\cos n\omega t+b_n\sin n\omega t) \tag{3.2}$$

Where

$$\begin{aligned} a_n &= \frac{1}{\pi}\int_0^{2\pi} z(t)\cos n\omega t\, d(\omega t) \qquad (n=0,1,2,\ldots) \\ b_n &= \frac{1}{\pi}\int_0^{2\pi} z(t)\sin n\omega t\, d(\omega t) \qquad (n=1,2,3,\ldots) \end{aligned} \tag{3.3}$$

Noting that the transfer function of the linear part in Figure 3.1 is given by

$$G(s)=G_1(s)G_2(s)G_3(s)=\frac{Ae^{-\tau s}}{s(s+\Gamma)} \tag{3.4}$$

The magnitude of *G(s)* for a sinusoidal input is

$$|G(j\omega)|=\frac{A}{\omega\sqrt{\omega^2+\Gamma^2}} \tag{3.5}$$

The magnitude $|G(j\omega)|$ decreases monotonically with increasing frequency ω, hence implying that *G(s)* acts as a low pass filter. We assume that all higher order harmonic components associated with

Equation (3.2) are filtered out by the linear part of the system. This assumption is reasonable because of the low pass property of *G(s)*. Similar assumptions are commonly made in control systems engineering for analysis and design of nonlinear time-varying systems. Naturally, if *G(s)* does not represent a good low pass characteristic then it is necessary to take into account any significant higher order harmonic components. This issue will be explored later in the Section 3.3. However, given the above assumption it follows that *z(t)* can be approximated by

$$\begin{aligned} z(t) &\approx \frac{a_0}{2} + a_1 \cos\omega t + b_1 \sin\omega t \\ &\approx \frac{a_0}{2} + \sqrt{a_1^2 + b_1^2}\, \sin(\omega t + \tan^{-1}\frac{a_1}{b_1}) \end{aligned} \tag{3.6}$$

The nonlinear element N_1 can therefore be quasi-linearised (Gelb and Velde, 1968) using the input and output relationships described by Equations (3.1) and (3.6). The DIDF is defined to be the complex ratio of the fundamental harmonic component of the output *z(t)* to the input *x(t)*, that is

$$N_1 = \frac{\sqrt{a_1^2 + b_1^2}}{D} \angle \tan^{-1}\frac{a_1}{b_1} \tag{3.7}$$

The stability of the closed-loop control system shown in Figure 3.1 is determined by the characteristic equation.

$$1 + N_1 G(j\omega) = 0 \tag{3.8}$$

or

$$G(j\omega) = -1/N_1 \tag{3.9}$$

$G(j\omega)$ and $-1/N_1$ can be plotted on the same complex plane as shown in Figure 3.2.

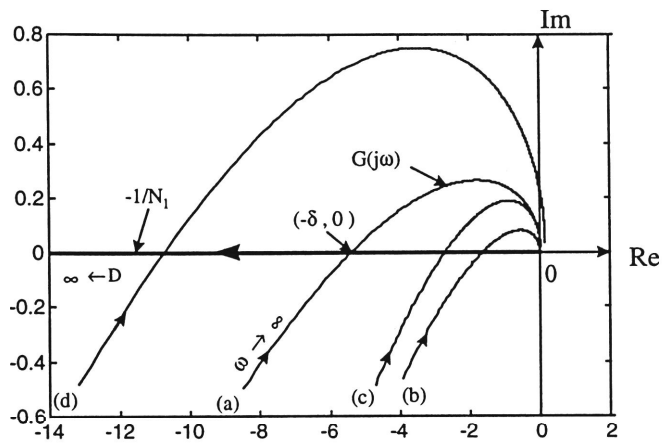

Figure 3.2 *Plots of $-1/N_1$ and $G(j\omega)$ locus on the complex plane.*

μ=155 Mb/s, ν=34 Mb/s.

(a) $A=860\ Mb/s^2$, $\Gamma=1.6\ 1/s, \tau=10\ ms$.

(b) $A=258\ Mb/s^2$, $\Gamma=1.6\ 1/s, \tau=10\ ms$.

(c) $A=860\ Mb/s^2$, $\Gamma=3.2\ 1/s, \tau=10\ ms$.

(d) $A=860\ Mb/s^2$, $\Gamma=1.6\ 1/s, \tau=20\ ms$.

The describing function method can be used to establish the following observations (Ogata, 1990):

1. If the $-1/N_1$ locus is enclosed by the $G(j\omega)$ locus then the closed-loop system is unstable (extended Nyquist criterion).

2. If the $-1/N_1$ locus and the $G(j\omega)$ locus intersect then the system output may exhibit a sustained oscillation or limit cycle. The amplitude of the limit cycle is given by the value of D on the $-1/N_1$ locus at the point of

intersection; the frequency of the sustained oscillation is also given by the value of ω on the $G(j\omega)$ locus at the point of intersection.

3.2.2 Single VC case

Let us now consider the DIDF analysis of the feedback control system shown in Figure 3.1. Using Equations (3.2) and (3.3) we compute the nonlinear output $z(t)$ as follows:

$$z(t) = \frac{2}{\pi}\alpha + \frac{4}{\pi}\cos\alpha \sin\omega t + \sum_{n=2,4,\ldots}^{\infty} \frac{4}{\pi n}\sin n\alpha \cos n\omega t + \sum_{n=3,5,\ldots}^{\infty} \frac{4}{\pi n}\cos n\alpha \sin n\omega t \tag{3.10}$$

where

$$\alpha = \sin^{-1}\frac{C}{D} \qquad (\alpha < \pi/2) \tag{3.11}$$

In the above equation $\alpha<\pi/2$ implies $C/D<1$, which is a necessary condition for a limit cycle to exist. This can be explained using Figure 3.3 as follows. When $C/D<1$ is satisfied, $x(t)$ will change its sign periodically. It follows that the buffer queue length $q(t)$ exceeds the queue threshold q_T from time to time because $x(t)=q_T - q(t)$. Consequently, the binary feedback $z(t)$ will change between 1 to -1 accordingly. However, when C/D is equal to 1, $x(t)$ will no longer cross the zero line and $q(t)$ is always less than q_T. As a result, the feedback $z(t)$ remains $+1$. Equation (3.10) indicates that the oscillation frequency can only be zero because $z(t)$ is a constant. It follows that there is no limit cycle in such a closed loop feedback system. The above analysis also applies to the situation where $C/D>1$ in which case $z(t)$ is $+1$.

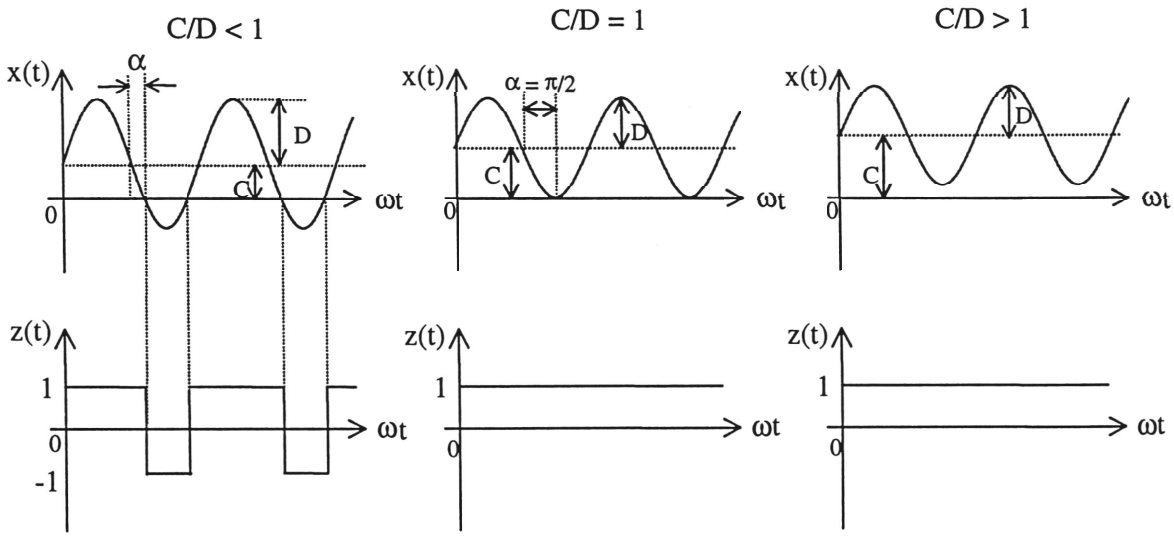

Figure 3.3 *The necessary conditions for limit cycle behaviour.*

We now derive the DIDF. Under steady state conditions the bias at the input $G_3(s)$ must be zero because of the integrating effect of the queue (Mitra, 1988). It follows that the ratio of *C/D* can be determined from a balance equation representing the fixed components around the closed-loop,

$$(\frac{2A}{\pi}\alpha+\Gamma v)\frac{1}{\Gamma}-\mu=0 \tag{3.12}$$

Combining Equations (3.11) and (3.12), we get

$$\alpha=\frac{\pi\Gamma}{2A}(\mu-v) \tag{3.13}$$

and

$$C=D\sin[\frac{\pi\Gamma}{2A}(\mu-v)] \tag{3.14}$$

The DIDF is given by

$$N_1 = \frac{4}{\pi D}\cos\alpha = \frac{4}{\pi D}\cos[\frac{\pi\Gamma}{2A}(\mu - v)] \tag{3.15}$$

We now study the system stability according to Figure 3.2. As the amplitude D increases from zero to infinity, the locus $-1/N_1$ will go from zero to negative infinity covering the entire negative real axis. On the other hand, as the frequency ω increases the $G(j\omega)$ locus will start from $-j\infty$ upwards across the negative real axis reaching the second phase. Therefore, the locus $G(j\omega)$ must intersect the locus $-1/N_1$. According to the extended Nyquist criterion (Ogata, 1990) the closed-loop system is stable. By substituting Equations (3.15) and (3.4) into Equation (3.8) the amplitude D and the frequency ω at the intersection can be determined approximately as

$$D \approx \frac{4A}{\pi\omega\sqrt{\omega^2 + \Gamma^2}}\cos[\frac{\pi\Gamma}{2A}(\mu - v)] \tag{3.16}$$

where

$$\omega \approx \sqrt{\Gamma/\tau} \qquad when \quad \omega > \Gamma \tag{3.17}$$

We now consider the stability of the limit cycle given by Equations (3.16) and (3.17). As shown in Figure 3.2 if the amplitude D increases slightly due to a slight disturbance the operating point of the system will move to the left hand side of the intersection $(-\delta, 0)$. According to the extended Nyquist criterion (Ogata, 1990) the system at this operating point is stable and the closed-loop system will force the amplitude D to decrease. Consequently, the operating point will be forced to move back towards the

intersection. Similarly, it can be shown that if the amplitude D decreases from the value at the intersection the closed-loop will force it to increase until it returns to the value given by Equation (3.16). It follows that the limit cycle is stable and the oscillation is sustained.

Equations (3.16) and (3.17) show that the amplitude of limit cycle will increase when the "gain" A increases or the round trip time delay τ increases. Similarly a decrease in the "damping" Γ will also cause the amplitude of limit cycle to increase. This can be shown graphically using Figure 3.2. When the time delay τ is increased the intersection will move to the left resulting in a greater δ. This in turn means that the amplitude of the limit cycle will increase. When the "gain" A is decreased or the "damping" Γ is increased the intersection will move to the right resulting in a smaller δ thus implying a smaller amplitude of oscillation.

3.2.3 Multiple VC case

We now extend the limit cycle analysis of a single VC to the more important multiple VC case by deriving the relationship between parameters such as; A, Γ, τ, J and the limit cycle behaviour in order to provide guidelines for the MS algorithm parameter selection. For simplicity let $\Gamma=\Gamma_i$ and $A=A_i$ $(i=1, 2, \ldots, J)$. The bias C becomes

$$(\frac{2A}{\pi}\alpha+\Gamma v_1)\frac{1}{\Gamma}+(\frac{2A}{\pi}\alpha+\Gamma v_2)\frac{1}{\Gamma}+\ldots+(\frac{2A}{\pi}\alpha+\Gamma v_J)\frac{1}{\Gamma}-\mu=0 \qquad (3.18)$$

From Equation (3.18), we have

$$\alpha=\frac{\pi\Gamma}{2AJ}(\mu-\sum_{i=1}^{J}v_i) \qquad (3.19)$$

Combining Equation (3.19) with Equation (3.11), we get

$$C = D\sin[\frac{\pi\Gamma}{2AJ}(\mu - \sum_{i=1}^{J} v_i)] \tag{3.20}$$

The DIDF is given by:

$$N_1 = \frac{4}{\pi D}\cos[\frac{\pi\Gamma}{2AJ}(\mu - \sum_{i=1}^{J} v_i)] \tag{3.21}$$

Similar to Equation (3.4), the linear part in Figure 2.3 has the form:

$$G(s) = \frac{A\sum_{i=1}^{J} e^{-\tau_i s}}{s(s+\Gamma)} \tag{3.22}$$

If the exponential function in Equation (3.22) is simplified using a first order polynomial approximation as $\tau_i s \to 0$ *(i=1, 2, ..., J),* we can rewrite Equation (3.22) as

$$G(s) \approx \frac{A\sum_{i=1}^{J}(1-\tau_i s)}{s(s+\Gamma)} \approx \frac{AJ(1-\frac{1}{J}\sum_{i=1}^{J}\tau_i s)}{s(s+\Gamma)} \tag{3.23}$$

Substituting Equations (3.21) and (3.22) into Equation (3.8), we have the following approximate solutions:

$$D \approx \frac{4AJ}{\pi\omega\sqrt{\omega^2+\Gamma^2}}\cos[\frac{\pi\Gamma}{2AJ}(\mu - \sum_{i=1}^{J} v_i)] \tag{3.24}$$

$$\omega \approx \sqrt{\Gamma\Big/(\frac{1}{J}\sum_{i=1}^{J}\tau_i)} \qquad when\ \ \omega > \Gamma \tag{3.25}$$

Using Equations (3.24) and (3.25) we can now discuss the relationship between the parameters and the oscillations behaviour.

3.2.3.1 Affect of gain A and damping Γ parameters

Similar to a single VC case, the amplitude of the limit cycle will increase when the "gain" A increases or the "damping" Γ decreases at the sources. The frequency of oscillation will increase when Γ increases.

3.2.3.2 Affect of VC transmission time delays

Analysis shows that the average time delay $\sum_{i=1}^{J} \tau_i / J$ plays an important role in the oscillation. It is interesting to note that it is not the longest time delay but the average time delay that determines the characteristics of the oscillation. An increase in the average time delay of the active VCs will cause an increase in the amplitude and a decrease in the frequency of the oscillation.

3.2.3.3 Affect of number of active VCs

When new connections are added, the frequency may either increase or decrease depending on the average time delay. However, the amplitude of oscillation will increase as the number of active VCs increase. Refer to Appendix B for a detailed proof.

3.3 Accuracy of DF approach

The DIDF analysis presented above is an approximate analytical method. It uses a sinusoid plus a constant bias to represent the waveform $x(t)$, which is the difference between the threshold q_T and the buffer queue

length *q(t)*. The DIDF method cannot predict the limit cycle accurately when the waveform *x(t)* differs greatly from a sinusoid plus a bias. Such a situation can occur when higher order harmonic components are present at the output of the nonlinear element. This situation reflects the case where the linear part, *G(s)*, is not characterised by an effective low pass filtering characteristic (Gelb and Velde, 1968). In particular, the second harmonic will play an important role if it cannot be filtered out by the linear part. We use examples to illustrate the affects of the second order harmonic component in order to assess the accuracy of DIDF.

Letting X_1 and X_2 represent the magnitude of the fundamental and the second order harmonic of z(t) respectively. From Equation (3.10) for the single VC case:

$$X_1 = \frac{4}{\pi}\cos\alpha \tag{3.26}$$

$$X_2 = \frac{2}{\pi}\sin 2\alpha \tag{3.27}$$

$$\text{Hence} \quad \frac{X_2}{X_1} = \frac{\frac{2}{\pi}\sin 2\alpha}{\frac{4}{\pi}\cos\alpha} = \sin\alpha \tag{3.28}$$

Substituting Equation (3.13) into Equation (3.28) we have

$$\frac{X_2}{X_1} = \sin\alpha = \sin[\frac{\pi\Gamma}{2A}(\mu - v)] \tag{3.29}$$

Clearly the higher the ratio of Γ/A the greater the X_2/X_1 ratio. In the worst case we choose the ratio of Γ/A close to $1/(\mu\text{-}\nu)$. It follows that the magnitude of the second order harmonic X_2 approaches the magnitude of the fundamental harmonic X_1 in $z(t)$ according to Equation (3.29). However, X_2 will be reduced when passing through the linear part of the system, which acts as a low pass filter. The decrease in the second order harmonic component of $x(t)$ can be estimated from Equation (3.5) and has the form:

$$\frac{|G(j2\omega_0)|}{|G(j\omega_0)|} = \frac{\sqrt{\omega_0^2 + \Gamma^2}}{2\sqrt{4\omega_0^2 + \Gamma^2}} \tag{3.30}$$

Where, ω_0 denotes the frequency of the fundamental harmonic. Figure 3.4 shows that $G(s)$ reduces the second order harmonic component by a factor of *50%* to *75%* in all possible frequencies. In the worst case where X_2 is close to X_1, the ratio of the second order harmonic to the fundamental in $x(t)$ is over *25%* which implies that the waveform $x(t)$ differs greatly from the assumption indicated in Equation (3.1) and causes poor DIDF accuracy. Clearly the DIDF accuracy can be improved by taking the second order harmonic component into account. The later is referred to as the refined DIDF method (Gelb and Velde, 1968). Unfortunately this adds considerable complexity to the calculation, which may not be justified in the case where an approximate solution is required given the other system unknowns and inaccuracies.

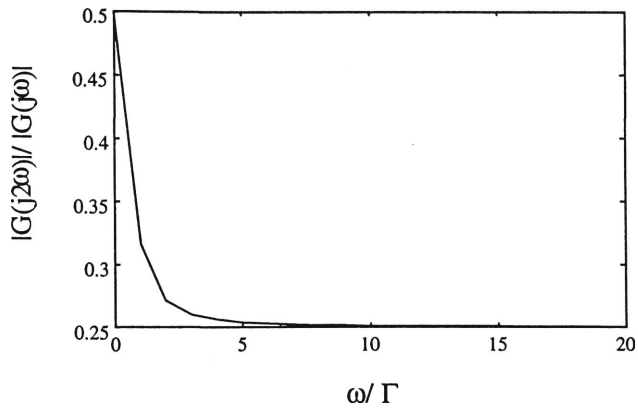

Figure 3.4 *The low pass efficiency of G(s).*

Figures 3.5 and 3.6 depict the DIDF and refined DIDF accuracy when compared with the simulation results. Note that we have shown in Chapter 2 that the SIMULINK implementation is consistent with results presented in (Bonomi, Mitra and Seery, 1995). Figure 3.5 shows how various values of the amplitude parameter "*A*" in the MS algorithm affect the amplitude and frequency of oscillation of the limit cycle as predicted by the DIDF and its refined version. SIMULINK is used for simulation of the nonlinear system for comparison with the analysis results. Figure 3.5 (in particular Figure 3.5 b) shows that the accuracy of a describing function depends on the value of *A:* the greater the value of *A* the better the accuracy. This is in agreement with above analysis. It is also evident that the refined DIDF provides a better approximation as expected. The results show that the DIDF analysis provides more accurate results in terms of the amplitude of oscillation when compared to the frequency of oscillation. This is fortuitous because the amplitude of oscillation is of primary concern as it impacts more significantly on the buffer occupancy. Figure 3.6 presents similar results where the damping ratio, "*Γ*" associated with the MS algorithm is varied.

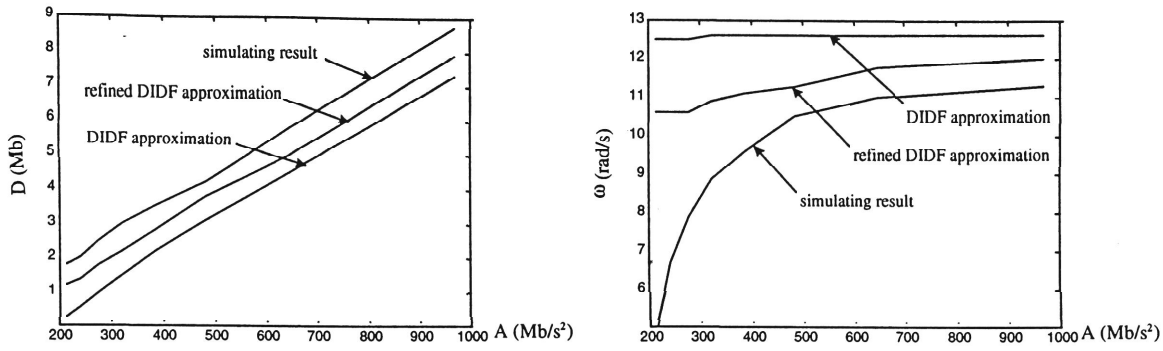

(a) *(b)*

Figure 3.5 *Various values of A for one VC. Γ=1.6 1/s, μ=155 Mb/s, ν=34Mb/s, τ=10 ms.*

(a)Various values of A versus the amplitude of queue oscillation.

(b)Various values of A versus the frequency of queue oscillation.

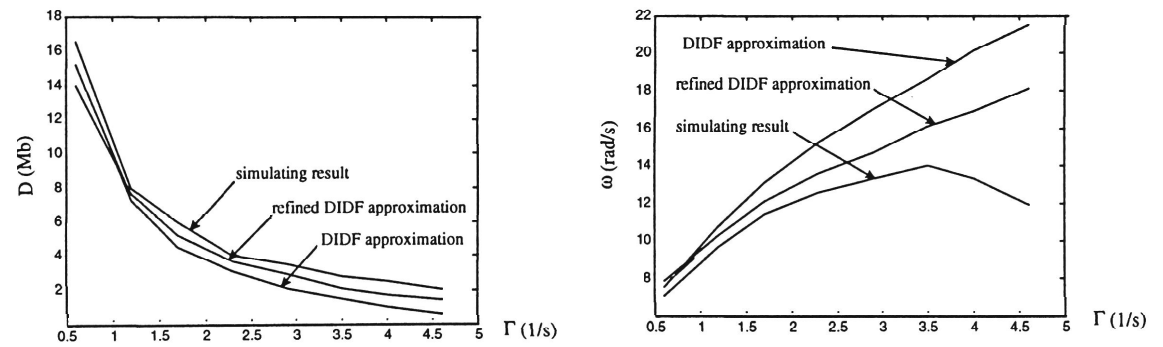

(a) *(b)*

Figure 3.6 *Various values of Γ for one VC. A=700 Mb/s², μ=155 Mb/s, ν=34 Mb/s, τ=10 ms.*

(a) Various values of Γ versus the amplitude of queue oscillation.

(b) Various values of Γ versus the frequency of queue oscillation.

3.4 Simulation Results

Simulations were carried out in order to demonstrate the relationship between average time delay of active VCs and the limit cycle behaviour associated with the multiple VC case. The results are depicted in Table 3.1, where the numbers of active VCs in each example are set to 20 while the individual time delays in each case are different. The last two columns of Table 3.1 show that the average time delays are exactly the same although the difference in individual time delays among the two groups of VCs is considerably different. It is interesting to note that in these cases the frequency and amplitude of oscillation are almost the same. There is generally good agreement between the DIDF analysis and the actual multiple VC SIMULINK implementation. This is particularly important, as the multiple VC case is rather difficult to analyse using time domain approaches (Gelb and Velde, 1968) thus demonstrating the usefulness of the DIDF analytical tool.

Table 3.1 *Comparison between DIDF estimates and SIMULINK results for many VCs. 20 VCs group of 4 VCs turn on at 0, 2, 4, 6 s.* A_i*=35 Mb/s*^{2}*;* Γ_i*=1.6 1/s;* μ*=155 Mb/s;* v_i*=4 Mb/s, for i=1,2,3,...,20.* $\tau_{g1}=\tau_i$ *for i=1,2,3,4,5.* $\tau_{g2}=\tau_i$ *for i=6,7,8,9,10.* $\tau_{g3}=\tau_i$ *for i=11,12,13,14,15.* $\tau_{g4}=\tau_i$ *for i=16,17,18,19,20.*

Time delay / Limit cycle characteristics		τ_{av}=2.5 ms τ_{g1}=1 ms τ_{g2}=2 ms τ_{g3}=3 ms τ_{g4}=4 ms	τ_{av}=5 ms τ_{g1}=2 ms τ_{g2}=4 ms τ_{g3}=6 ms τ_{g4}=8 ms	τ_{av}=10 ms τ_{g1}=4 ms τ_{g2}=8 ms τ_{g3}=12 ms τ_{g4}=16 ms	τ_{av}=15 ms τ_{g1}=6 ms τ_{g2}=12 ms τ_{g3}=18 ms τ_{g4}=24 ms	τ_{av}=15 ms τ_{g1}=1 ms τ_{g2}=10 ms τ_{g3}=5 ms τ_{g4}=44 ms
DIDF analysis	ω (rad/s)	25.3	17.9	12.6	10.3	10.3
	D (Mb)	1.3	2.7	5.3	8.0	8.0
SIMULINK	ω (rad/s)	22.8	16.2	11.9	9.6	9.6
	D (Mb)	1.6	3.2	6.2	9.4	9.1

3.5 Conclusion

In this chapter we analysed the performance of the MS algorithm with the network model derived in Chapter 2. The analysis was carried out in Laplace domain instead of time domain and this contrasts against the approach taken by Bonomi, Mitra and Seery (1995). The significant advantage of using the frequency domain rather than the time domain is that we can easily analyse the multiple VC case. An approximate steady state solution is obtained using Describing Function under the linear buffer assumption. The results show that the amplitude of the limit cycle will increase following an increase in the "gain" A or a decrease in the "damping" Γ. The average time delay of the active VCs plays an important role in the oscillation, that is, its increase will cause an increase in the amplitude of the oscillation while a decrease in the frequency of the oscillation. The amplitude of oscillation will also increase as the number of active VCs increases.

The accuracy of the proposed DF approach was investigated by harmonic analysis and examined using SIMULINK package. It was found that the accuracy depends on the ratio of Γ/A. The higher the ratio, the poorer the accuracy. The reason for the poorer accuracy arises from the fact that buffer queue length oscillation becomes nonsinusoidal (in the sense that it contains higher order harmonics) for high values of Γ/A. The proposed analysis will be used as a guideline for the algorithm design in the next Chapter.

Chapter 4

Design of a Modified MS Algorithm (MMS)

4.1 Introduction

As mentioned in Chapter 1, the goal of ABR flow control is to enable the network to allocate the available bandwidth fairly and efficiently among ABR users. In this section, we will describe efficiency and fairness issues quantitatively in order to enhance the MS algorithm accordingly.

4.1.1 Efficiency

An important network performance criterion is the issue of achieving high throughput and low switch queuing delay. However, there is a tradeoff between the throughput and delay (Yang and Reddy, 1995, Jain, Ramakrishnan and Chiu, 1988). As shown in Figure 4.1, when the load is lower than the link capacity the buffer is empty thus there will be no delay at the switch. The link utilisation remains low and the throughput will go up as the load increases. When the load reaches the link capacity the link utilisation will be 100% and the throughput will stop increasing. However, the queue will start to grow and the delay will rise very fast. Moreover, cells will be dropped if the queue length eventually exceeds the available buffer size. Consequently, the throughput will go down since some cells can not reach the destination.

From the above discussion the optimal operating point should clearly be at the knee point as shown in Figure 4.1, where utilisation is close to 100% and the delay is acceptable. An appropriately designed flow control scheme should ensure that users adapt their traffic load to let the network operate around the knee point (Yang and Reddy, 1995, Jain, Ramakrishnan and Chiu, 1988).

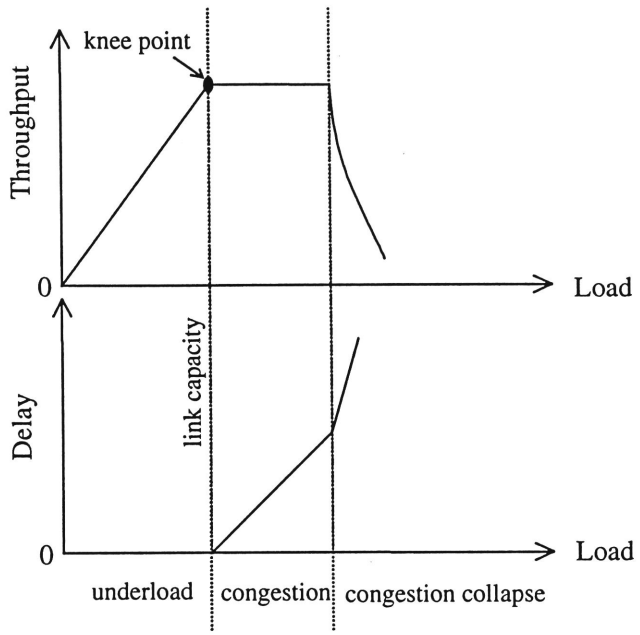

Figure 4.1 *Network performance with varying traffic load (Jain, Ramakrishnan and Chiu, 1988).*

4.1.2 Fairness

Fairness is a desirable objective of the ABR service. At an intuitive level, any bandwidth allocation scheme is fair if it does not offer different treatment to different connections. As an example of fairness criteria, the ATM Forum (1996) recommended five definitions of fairness measures as proposed by Sathaye (1994), Yin (1994) and Hughes (1994), these include:

4.1.2.1 Max-Min

The available bandwidth on a given link is equally shared among n connections. The rate associated with each active connection is given by

$$B_i = B / n \qquad (i = 1, 2, \ldots, n) \qquad (4.1)$$

where n is the number of active connections to which the given link is a bottleneck. B is the available bandwidth for these ABR connections. B represents the difference between the total available bandwidth for all connections and the sum of the bandwidth of connections bottlenecked elsewhere. Consider the example given in Figure 4.2 explaining the Max-Min fairness criterion. The network contains two links, both have a *120 Mb/s* link capacity. The first link *L1* is shared by the four sources, S1, S2, S3 and S4, and the second link *L2* is shared by three sources, S2, S5 and S6. On link *L1*, the four connections share the bandwidth equally and each gets a share of *30 Mb/s*. On link *L2*, each of the three connections should have a share of *40 Mb/s*. However, *L2* is not a bottleneck for S2, which is only allocated *30 Mb/s* bandwidth on link *L1*. According to Max-Min criteria, the available bandwidth for the connections bottlenecked on *L2* is *120-30=90 Mb/s*. It is equally shared among the rest of two connections, each has a share of *45 Mb/s*. Therefore, the Max-Min allocation for the source S1, S2, ..., S6 is *30, 30, 30, 30, 45, 45 Mb/s* respectively.

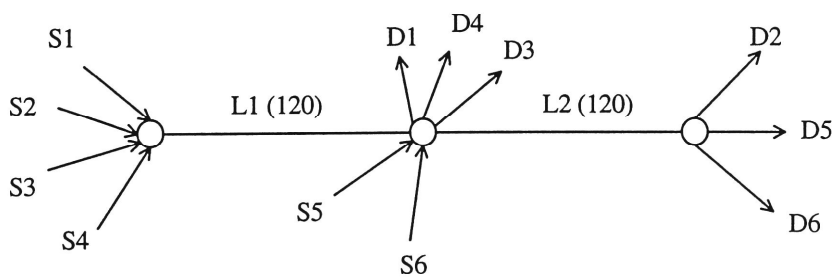

Figure 4.2 *Example network for Max-Min share.*

4.1.2.2 Minimum Cell Rate (MCR) plus equal share

Each active source is first allocated its MCR. Then, the rest of the bandwidth is determined using the Max-Min criteria and is added on as follows.

$$B_i = MCR_i + (B - \sum_{j=1}^{n} MCR_j)/n \qquad (i = 1, 2, \ldots, n) \qquad (4.2)$$

4.1.2.3 Maximum of MCR or Max-Min share

The share of each connection is determined using the larger bandwidth between the MCR and the Max-Min share.

$$B_i = \max(MCR_i, B/n) \qquad (i = 1, 2, \ldots, n) \qquad (4.3)$$

4.1.2.4 Allocation proportional to MCR

The bandwidth allocated to each connection is proportional to its MCR.

$$B_i = B*(MCR_i / \sum_{j=1}^{n} MCR_j) \qquad (i = 1, 2, \ldots, n) \qquad (4.4)$$

4.1.2.5 Weighted allocation

The bandwidth allocated to each connection is proportional to its weight.

$$B_i = B*(W_i / \sum_{j=1}^{n} W_j) \qquad (i = 1, 2, \ldots, n) \qquad (4.5)$$

Where W_i is a pre-determined weight for connection i.

The appropriateness of a fairness criterion depends on the environment in which it is used. The Max-Min criterion applies only to the case where all connections are equally weighted and the minimum cell rate (MCR) is zero. The criterion of Allocation Proportional to MCR does not apply if there are connections with zero MCR. It should also be pointed out that

the above definitions of fairness only apply to greedy sources not bursty sources.

The concepts of efficiency and fairness have been described quantitatively. In Section 4.2 we study how to achieve the optimal performance in the system considered. Simulation results are given in Section 4.3 followed by the conclusion in Section 4.4.

4.2 MMS algorithm design

The analytical results obtained in Chapter 3 indicate that a stable limit cycle exists in the system shown in Figure 3.1 if $\alpha<\pi/2$. Similarly for multiple connections it can be shown from Equation (3.18) that the necessary condition for sustained limit cycle behavior occurs when:

$$\frac{\Gamma}{AJ}(\mu - \sum_{i=1}^{J} v_i) < 1 \tag{4.6}$$

The queue limit cycle characteristics depend on the "gain" A, the "damping" Γ and the transmission time delay. Further, the amplitude of oscillation of the queue length rises as the number of active VCs increases.

Steady state oscillation-free operation will exist if

$$\frac{\Gamma}{AJ}(\mu - \sum_{i=1}^{J} v_i) \geq 1 \tag{4.7}$$

which can be used as a guideline for system design. The gain A and damping Γ should be chosen appropriately to satisfy Equation 4.7 in order to avoid the limit cycle. Although Equation 4.7 was obtained assuming the linear buffer characteristics the above necessary condition of oscillation-free operation can be extended to the case where the buffer is empty and its input rate is less than or equal to the service rate μ. The reason is that the feedback information and source rate remain unchanged under the oscillation-free operation during steady state. It follows that the buffer input rate Φ_Σ (that is, arrival rate), being the sum of all active VC's rates, can be obtained from Equation (2.8) as follows:

$$\Phi_\Sigma = \sum_{i=1}^{J}(\nu_i + \frac{A}{\Gamma}) = \frac{AJ}{\Gamma} + \sum_{i=1}^{J}\nu_i \tag{4.8}$$

When Φ_Σ is less than or equal to the buffer service rate μ the following equation can be obtained from Equation (4.8)

$$\frac{AJ}{\Gamma} + \sum_{i=1}^{J}\nu_i \le \mu \tag{4.9}$$

It is equivalent to Equation (4.7). Therefore, Equation (4.7) is the necessary condition of oscillation-free operation for both empty and nonempty buffer circumstances and can be applied to not only the linear buffer model but also the empty buffer case.

We now discuss the selection of the parameters related to the optimal operation point. Equation (4.8) shows that the buffer input rate is determined only by the "gain", the "damping" and the user's expectation of minimum bandwidth during the system's steady state. The higher the ratio A/Γ the higher the buffer input rate Φ_Σ. When Φ_Σ is equal to the

buffer service rate, that is, $\Phi_\Sigma=\mu$, the network utilisation reaches *100%* without causing any buffer queue delay. This corresponds to the point on the knee as discussed in the last section. The optimal operating point should be less but close to the knee point. Using an additional parameter *k* to describe the percentage of link utilisation we have

$$\Phi_\Sigma = k\mu \tag{4.10}$$

Thus, the knee point is achieved when *k=1*. However, for application *k* should be less than but close to *1* in order to achieve a near maximum link utilisation while avoiding oscillation. The value of A/Γ corresponding to the near optimal operating point can be obtained by combining Equations (4.8) and (4.10):

$$\frac{A}{\Gamma}=\frac{1}{J}(k\mu-\sum_{i=1}^{J}\nu_i) \tag{4.11}$$

Using the near optimal value, the rate of each source in steady state has the following expression.

$$\Phi_i=\nu_i+A/\Gamma=\nu_i+(k\mu-\sum_{j=1}^{J}\nu_j)/J \tag{4.12}$$

Note that Equation (4.12) meets the second fairness criterion, the so called MCR plus equal share criterion (refer to Subsection 4.1.2.2). The reasons are as the follows:

(i) The user's expectation of minimum bandwidth ν_i in Equation (4.12) captures the MCR in Equation (4.2).

(ii) The targeted bandwidth $k\mu$ in Equation (4.12) matches the available bandwidth B in Equation (4.2).

(iii)The number of active connections J in Equation (4.12) is n in Equation (4.2).

Therefore, a near optimal performance and fairness will be achieved by choosing the value of A/Γ according to Equation (4.11).

Equation (4.11) shows that the near optimal A/Γ ratio is not a constant because it depends on the number of active VCs. If the design is oscillation-free for a small number J of active VCs, a sustained queue oscillation will occur when J increases resulting in the satisfaction of the oscillation condition given by Equation (4.6). On the other hand, if the design is oscillation-free for a large J, the buffer input rate Φ_Σ will be far less than the link capacity μ, which will result in wasted bandwidth when J decreases. Hence the optimal A/Γ ratio will be a time varying parameter.

On the basis of the above analysis a new feedback control strategy can be developed and applied to the MS algorithm to achieve a near optimal performance during steady state operation. It will be referred to as modified MS algorithm (MMS). Depending on the number of active VCs the ratio A/Γ must be changed appropriately in order to maintain the system near its optimal operating point. That is, the sources should be informed about the number of active VCs and the user's expectation of minimum bandwidth whenever J varies. If the binary feedback indicates no congestion, each source increases its rate using the optimal parameters A^+/Γ^+ based on Equation (4.11). However, if congestion occurs each

source should decrease its rate using a different ratio denoted by A^-/Γ^-. The optimal choice of A^-/Γ^- is a difficult issue involving transient state analysis, which can be a research topic in the future. In the next section the effects of A^-/Γ^- on the maximum queue length will be demonstrated using simulation examples.

4.3 Simulation Results

This section presents design examples and simulation results in order to illustrate and examine the performance of the MMS algorithm. We consider three VCs *(J=3)* in which the source rates are adapted by the MMS algorithm. VC1 turns on at time 0, VC2 at *2.5 s* and VC3 at *6 s*. A time-varying ratio of A^+/Γ^+ is used where A^+ changes with time while Γ^+ remains fixed for simplicity of implementation. From Equation (4.11) we obtain

$$A^+(t) = \begin{cases} 362\ Mb/s^2, & J=1\ \ for\ t<2.5s \\ 127\,Mb/s^2, & J=2\ \ for\ 2.5s<t<6s \\ 48\,Mb/s^2, & J=3\ \ for\ t>6s \end{cases} \tag{4.13}$$

The parameter k in Equation (4.11) is set to *0.95*, which implies a target of *95%* link utilisation during steady state operation. Figure 4.3 (a) shows the simulation result obtained from MS algorithm which has a constant gain $A=362\ Mb/s^2$ (as specified by Bonomi, Mitra and Seery, 1995). Figure 4.3 (b) depicts the result of MMS algorithms, which has a time-varying gain.

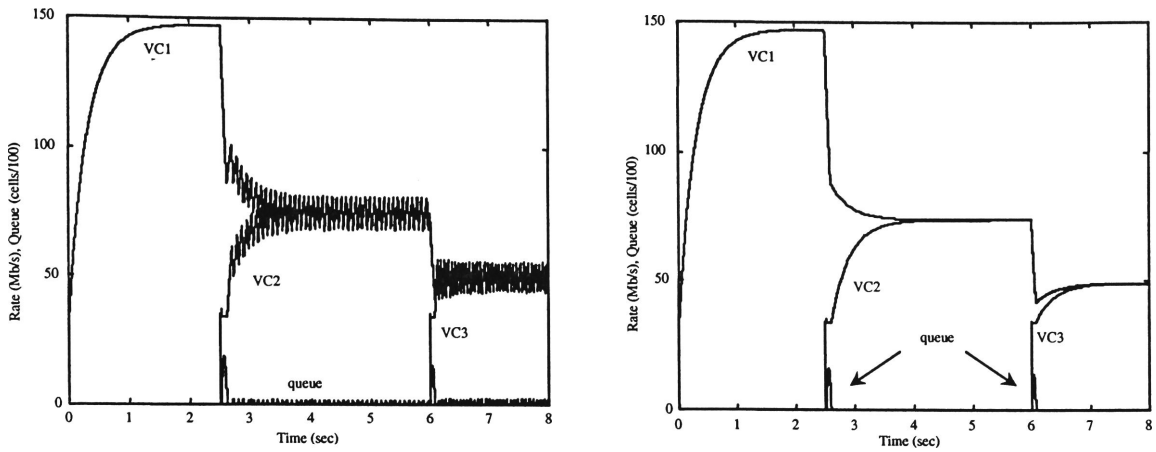

Figure 4.3 *VC1, VC2 and VC3 turn on at 0, 2.5 s and 6 s. Γ=3.2 1/s, μ=155 Mb/s, τ_1=10 ms, τ_2=8 ms, τ_3=4ms, $\nu_1=\nu_2=\nu_3$=34 Mb/s, q_T=6.5 cells. k=0. 95.*

(a) MS algorithm. A≡362 Mb/s^2.

(b) $A^+(t)$=362 Mb/s^2 for J=1, $A^+(t)$=127 Mb/s^2 for J=2 and $A^+(t)$=48 Mb/s^2 for J=3, A^-≡362 Mb/s^2.

Figure 4.3 (a) shows that the MS algorithm starts to oscillate after the second VC turns on. Figure 4.3 (b) shows that the MMS algorithm achieves optimal performance in the steady state sense and further it can be noted that:

i) The buffer remains empty except during the transient periods.

ii) The expected link utilisation is achieved.

iii) Active VCs equally share the available bandwidth during steady state operation.

Having considered the steady state performance we now study the transient state of the MMS algorithm. Figure 4.3 (b) shows that the switch queue builds up only during the transient state as a result of adding

new VCs. For example, the target bandwidth of *147 Mb/s* is occupied by VC1 before VC2 is added. When VC2 turns on at *2.5s*, the rate of VC2 step up to the bandwidth of *34 Mb/s,* which is the minimum bandwidth expected by a user. Thus, the sum of the two bandwidths is greater than the link capacity, *155 Mb/s,* and the queue builds up. Once the threshold is exceeded, the source will reduce its rate using the rate decrease gain A^-. A similar situation occurs at *6s* when VC3 becomes active.

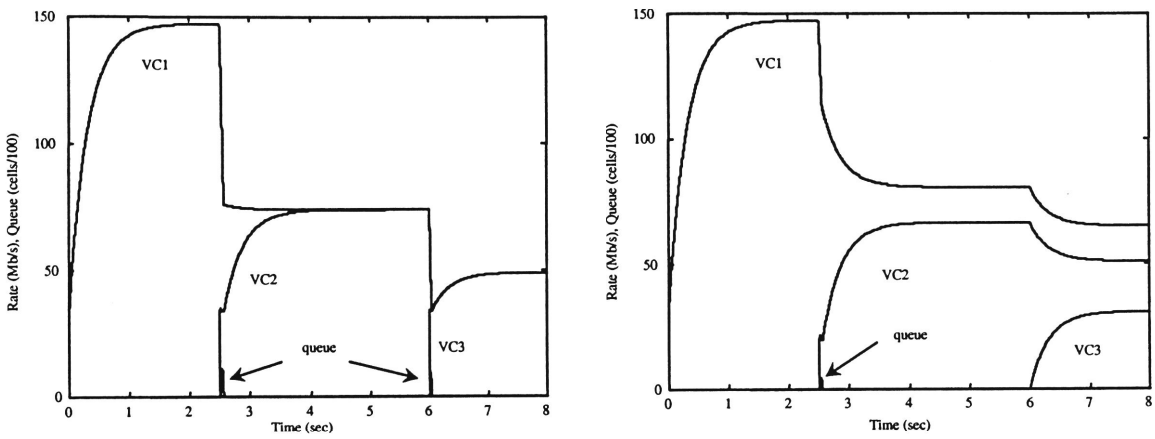

Figure 4.4 *VC1, VC2 and VC3 turn on at 0, 2.5 s and 6 s.* Γ*=3.2 1/s,* μ*=155 Mb/s,* τ_1*=10 ms,* τ_2*=8 ms,* τ_3*=4ms, k=0.95. Using MMS algorithm.*

(a) $\nu_1=\nu_2=\nu_3=34$ *Mb/s,* $A^-\equiv 1000$ *Mb/s*^{2}, $A^+(t)$ *is same value as Figure 4.3 (b).*

(b) $\nu_1=34$ *Mb/s,* $\nu_2=20$ *Mb/s,* $\nu_3=0$, $A^+(t)=362$ *Mb/s*^{2} *for J=1,* $A^+(t)=149$ *Mb/s*^{2} *for J=2 and* $A^+(t)=99$ *Mb/s*^{2} *for J=3,* $A^- \equiv 362$ *Mb/s*^{2}.

Simulation tests were also carried out in order to investigate the effects of the rate decrease gain A^- and the user-expected minimum bandwidth ν_i on the transient state behavior of the network. The results are given in Figure

4.4, where both the traffic conditions and parameters are the same as for the simulation results depicted in Figure 4.3 (b), except that the decreasing gain $A^{-}=1000\ Mb/s^2$. The decreasing gain is greater than the one used previously. Comparison of Figure 4.3 (b) with Figure 4.4 (a) demonstrates that the maximum queue length is reduced from *1564* cells to *1106* cells. This is a very important result because it demonstrates that a higher A^{-} can be used for reducing the maximum queue length during congestion.

We now study the relationship between the minimum bandwidth and the queue length and consider the case where each of the three sources have different minimum bandwidth requirement, *34 Mb/s, 20 Mb/s* and zero as shown in Figure 4.4 (b). When VC2 is turned on, congestion occurs resulting in the maximum queue length of *432* cells. However, when VC3 is added at *6s*, no queue occurs because of zero minimum bandwidth requirement. In terms of fairness all three VCs still achieve an acceptable allocation of bandwidth.

From the simulation results it can be concluded that a low minimum bandwidth ν can also lead to much smaller queue lengths during congestion. Although ν is specified by the source and cannot be altered during the connection it is still possible to use a low rate at the beginning of a transmission such that the queue length is reduced.

4.4 Conclusion

In this chapter we modified the MS algorithm by developing an analytical expression for choosing the near optimal parameters. The MMS

algorithm meets the efficiency and fairness criteria by replacing the constant gain with a time-varying gain such that the binary feedback system can be maintained at the optimal operating point during steady state. Simulation results show that the MMS algorithm results in oscillation-free operation while fairness is maintained. Further, high link utilisation during steady state is achieved. The queue only builds up during initial transient time. Simulation tests were also carried out to demonstrate the effects of various rate decrease gain A^- and user-expected minimum bandwidth v. The results indicate that a larger A^- can be used for reducing the maximum queue length in the transient state while the network performance remains unchanged during the steady state operation. A lower starting rate can also lead to much smaller queue lengths during congestion. Therefore, the buffer size can be reduced using the MMS algorithm considerably.

Chapter 5

Performance of the MS and Proposed MMS Algorithms with Bursty ABR Sources and VBR/CBR Background Traffic

5.1 Introduction

In the previous chapters for simplicity reasons we assumed that all the link capacity is available for ABR service. In practice, however, there are also constant bit rate (CBR) and variable bit rate (VBR) traffic in ATM networks because ATM supports various traffic types. CBR service is used as emulated circuits for fixed bandwidth real-time applications, such as telephone and videoconferencing, where cells or packets are delivered with strictly bounded end-to-end cell delays and delay variations. VBR services offer connections up to a peak cell rate for variable bandwidth real-time or non-real-time applications such as compressed video and multimedia applications, where cells are delivered with a specified cell loss ratio that is bounded as required by the different applications. Because of the specified requirements CBR and VBR traffic has a higher priority than ABR traffic. ABR is designed to use the bandwidth that is left by CBR and VBR. The purpose, of course, is to increase the link utilisation without affecting the quality of the service for CBR and VBR connections. Because VBR traffic fluctuates from time to time the available bandwidth for ABR traffic is time varying.

In this chapter we will investigate the performance of the MS and the MMS algorithm under more realistic traffic conditions by taking the bandwidth variations into account. In addition, we will also study the effect of bursty sources in order to see if there is any stability problem or degradation in terms of oscillation. Section 5.2 describes an ABR traffic model, which has a bursty source. Simulation studies are reported in Section 5.3 illustrating the performance characteristics of the MS and the MMS algorithm under various traffic conditions. Section 5.4 concludes the chapter.

5.2 ABR Traffic Model

Greedy sources have been used in previous chapters in order to simplify the evaluation and improvement of the performance of the feedback flow control for ABR service. In practical applications ABR traffic sources are more complicated than the assumed greedy source traffic. For example, after sending a request to a server a client has generally to wait for some time before sending the next request. As a result, most of the data traffic on a network is expected to be bursty on-off sources (Jain *et al.*, 1995).

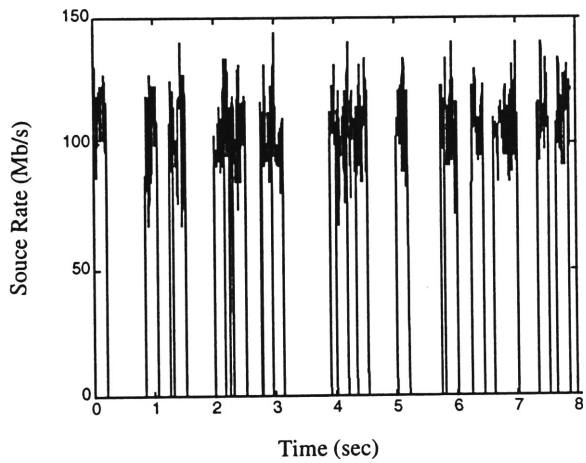

Figure 5.1 *An on-off source with intensity parameter* λ_1*=3,* λ_2*=5000 and a packet=50 cells.*

A Poission counting process is used for describing the bursty traffic (Pitts and Schormans, 1996, Liu, Anido and Chicharo, 1995) as follows.

$$P(N=n)=\frac{(\lambda_1 t)^n}{n!}e^{-\lambda_2 t} \qquad n=0,1,2,.... \tag{5.1}$$

where n is the number of bursts in the time interval (0, t) and λ_1 is the intensity parameter. In a bursty state, the number of packets is also a Poisson counting process with intensity parameter λ_2. An example of source traffic with intensity parameter $\lambda_1=3$ and $\lambda_2=5000$ is shown in Figure 5.1.

Considering the on-off characteristics of the traffic generated by a source, the rate calculated by the MS or the MMS algorithm is an upper bound of the cell transmission rate, known as the allowed cell rate. We assume that the formula used to calculate the allowed cell rate at each source is the same as that for greedy source. A source buffer is necessary to avoid cell loss when the cell arrival rate is greater than the allowed cell rate. The cell transmission rate of each ABR source can be described as follows:

$$\phi_s(t) = \begin{cases} y(t) & \text{if } q_s(t) = 0 \text{ and } y(t) < \phi(t), \\ \phi(t) & \text{others} \end{cases} \tag{5.2}$$

where $\phi_s(t)$ is the cell transmission rate, $y(t)$ is the rate at which the cells arrive at the source, $q_s(t)$ is the queue length at the source buffer and $\phi(t)$ is the allowed cell rate calculated by the MS or the MMS algorithm. Equation (5.2) shows that when the source buffer is empty, $q_s(t)=0$, and the allowed cell rate, $\phi(t)$, is greater than the arrival rate $y(t)$ the incoming cells will be transmitted immediately. Otherwise, these cells will be queuing up and sent at the allowed cell rate $\phi(t)$. Similar to the buffer at the distant switch, the source buffer can be described as:

$$\frac{d}{dt}q_s(t) = \begin{cases} y(t) - \phi_s(t) & if\ q_s(t) > 0 \\ [y(t) - \phi_s(t)]^+ & if\ q_s(t) = 0 \end{cases} \tag{5.3}$$

where the $[\ ]^+$ is defined by Equation (2.2) and captures the fact that the buffer level is always non-negative. The block diagram for the above bursty source is shown in Figure 5.2 where a single VC is considered together with the MS algorithm.

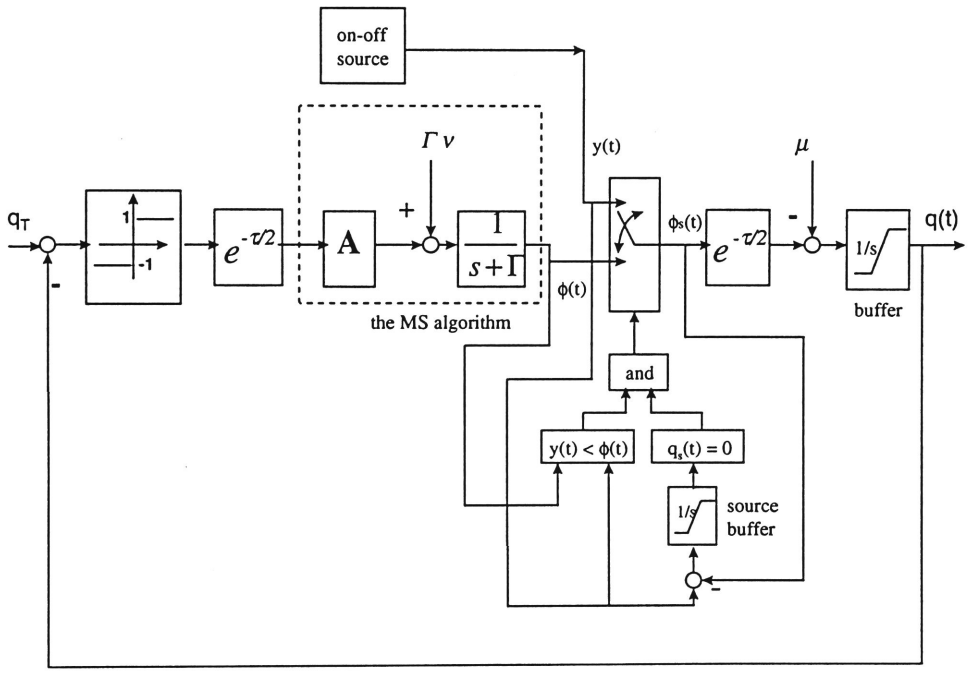

Figure 5.2 *A block diagram of a single VC binary feedback flow control system with bursty source using the MS algorithm.*

5.3 Simulation Results

In this section we present simulation results and illustrate the performance of binary feedback system, which are controlled by the MS or the MMS algorithm under the influence of the bursty sources. We first consider the case where bursty ABR sources use all the link capacity, that is, the whole bandwidth is available for the ABR sources. We then study the case where the VBR/CBR background traffic is added and the bandwidth available for ABR traffic is time varying.

5.3.1 Bursty ABR sources

In this subsection we only consider bursty ABR sources similar to that shown in Figure 5.1. We assume that there are three sources and they are all use the same ratio of $A(t)/\Gamma$ conforming to the fairshare design rule proposed by Bonomi, Mitra and Seery (1995).

Simulation results for MS and MMS algorithm are shown in Figure 5.3 and Figure 5.4, respectively. We first consider the MS algorithm. The virtual connection VC1 is turned on at time *0*, VC2 is added in at *2.5s* and VC3 at *6s*. Parameters used in the simulation are summarised in Figure 5.3 caption. Because the bursty source rate is always less than the queue service rate, *155 Mb/s,* at the distant switch buffer as shown in Figure 5.1, no congestion occurs during the period *(0, 2.5s).* However, the queue of the distant switch buffer starts to build up as the number of connections increases implying that the rate for the cell arriving at the buffer exceeds the link capacity.

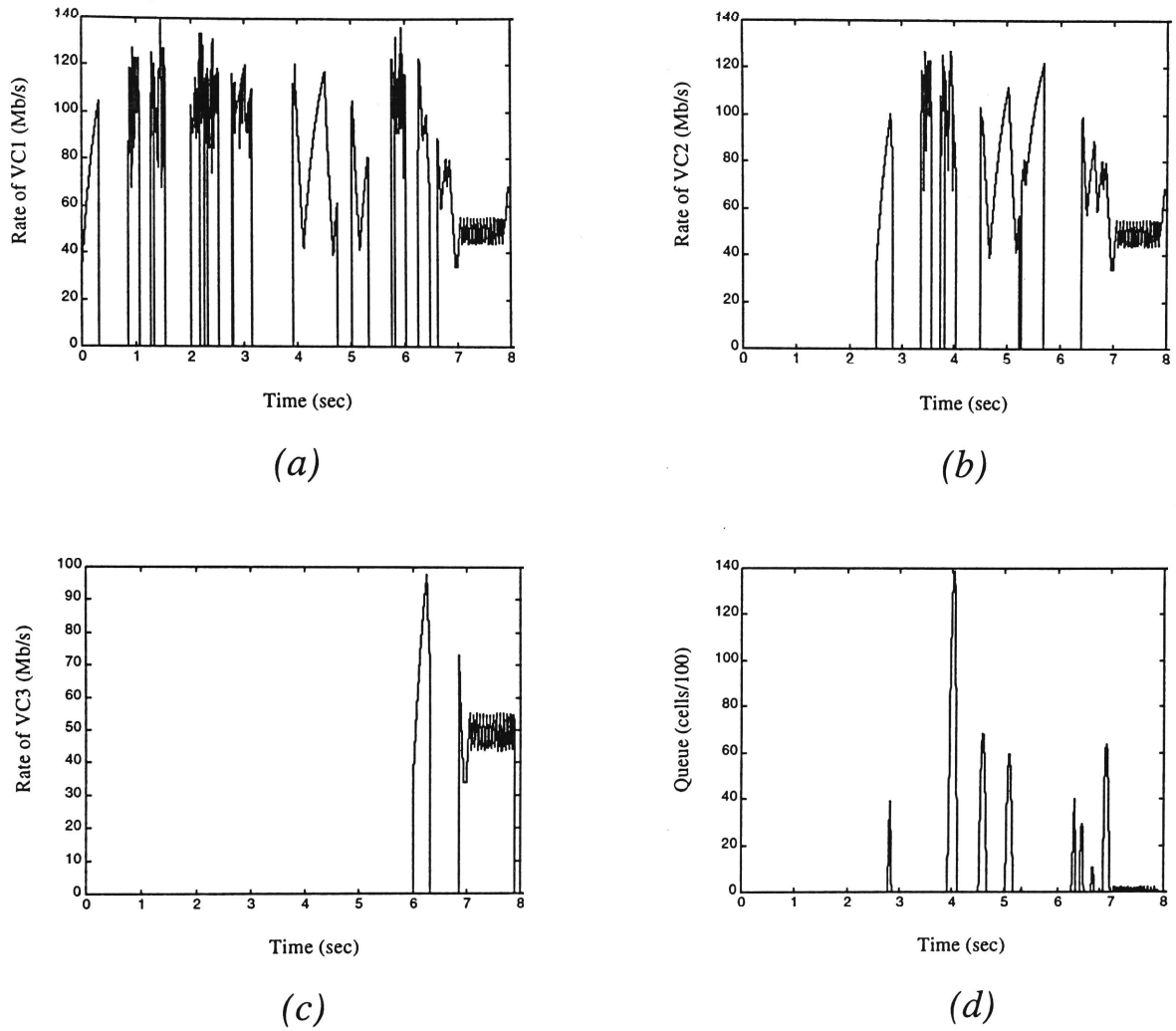

Figure 5.3 *The performance of the MS algorithm under bursty sources. VC1, VC2 and VC3 turn on at 0, 2.5 s and 6 s.* Γ*=3.2 1/s,* μ*=155 Mb/s,* τ_1*=10 ms,* τ_2*=8 ms,* τ_3*=4 ms,* $\nu_1=\nu_2=\nu_3$*=34 Mb/s. Three sources have the same intensity parameters as in Figure 5.1.*

The high queue length at the distant switch buffer in Figure 5.3 (d) is caused mainly by the large difference between the allowed cell rate and the cell transmission rate. Figure 5.3 (a) shows that during the period *(3s - 4s)* the rate of VC1 is zero for sometime during which period VC2 uses the link exclusively. As explained earlier, the distant switch is

underloaded and no congestion occurs because the arrival cell rate is less than the link capacity as shown by Figure 5.1. During this period (that is, 3-4 sec) the allowed cell rates for both VC1 and VC2 keep increasing because the feedback indicates no congestion. The transmission rate for VC1 remains zero before the next arrival on-state in VC1 at 4s. The allowed cell rate for VC1 reaches 113 Mb/s at 4s and allows the cell transmission rate of VC1 to jump to 113 Mb/s from zero when the on-state in VC1 arrives. Consequently, this large step increase in rate of VC1 leads to overload at the distant switch while the source of VC2 stays in its on-state.

The MMS algorithm performance is shown in Figure 5.4, where parameters used in the simulation are the same as in Figure 5.3 except that the gain A is time varying. A decreases as the connection number increases. As a result the upper limit of the cell transmission rate (allowed cell rate) at each source is decreased. The sum of the allowed cell rates of the three VCs is equal to the target bandwidth in steady state and no congestion will occur. This can be clearly seen in Figure 5.4 (d), where congestion only occurs in the transient state when a new VC is added in. Moreover, the MMS algorithm also achieves considerable improvement on maximum queue length. The maximum queue length is only *177* cells for the MMS algorithm as shown by Figure 5.4 (d). By comparison Figure 5.3 (d) shows that the maximum queue length for the MS algorithm is *13860* cells, which is much higher than that of the MMS algorithm.

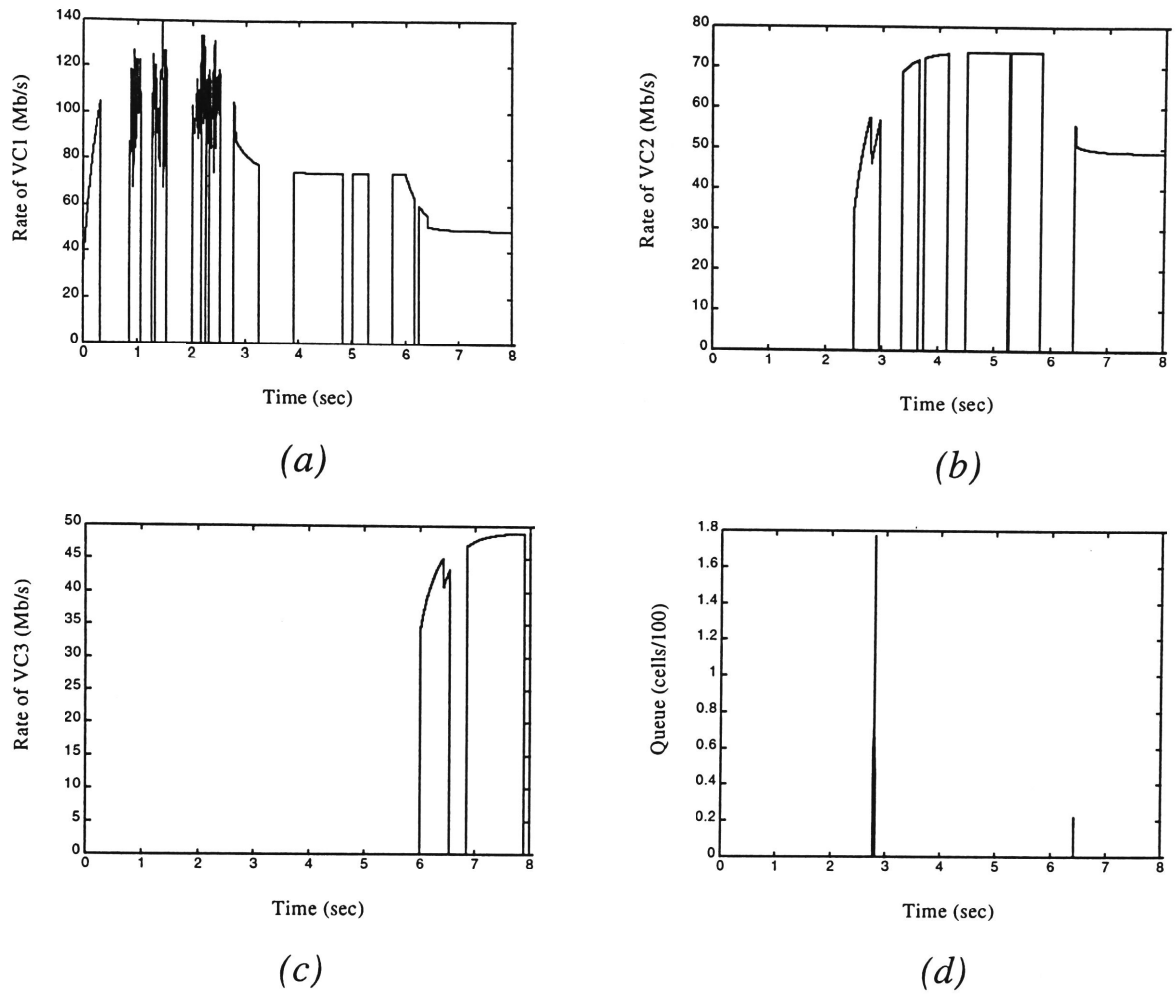

Figure 5.4 *The performance of the MMS algorithm under bursty sources. VC1, VC2 and VC3 turn on at 0, 2.5 s and 6 s. Parameters used in this simulation are same as in Figure 5.3 except three sources are adapted by the MMS algorithm, k=0.95, $A^+(t)$=362 Mb/s^2 for J=1, $A^+(t)$=127 Mb/s^2 for J=2 and $A^+(t)$=48 Mb/s^2 for J=3, A^- ≡362 Mb/s^2.*

A use-it-or-lose-it policy can be used in bursty traffic situation (ATM Forum, 1996). The allowed cell rate assigned to a connection will be reduced when its transmitting rate is significantly below the allowed level. The objective is to ensure that the allowed cell rate is maintained reasonably close to the cell transmission rate, which will reduce the step increase in the incoming rate from underload to overload at switches. Consequently, the intensity of congestion will be reduced. However, the

use-it-or-lose-it behaviour may cause unfairness if some of the sources do not implement the policy. These sources will obtain higher allowed cell rates (ATM Forum, 1996).

Use-it-or-lose-it behaviour can be achieved by different methods as discussed by Jain *et al.* (1996). For simplicity we implement it by modifying Equation (2.4) in the MS algorithm as follows:

$$\frac{d}{dt}\phi(t) = -\Gamma[\phi(t) - v] + Am(t) \tag{5.4}$$

$$m(t) = \begin{cases} -1 & if \quad [q_T - q(t - \tau/2)] < 0 \\ & \quad or \quad \phi(t) > \phi_s(t), \\ +1 & others \end{cases} \tag{5.5}$$

Equations (5.4) and (5.5) show that the allowed cell rate $\phi(t)$ in an ABR source is decreased when the queue length $q(t)$ at the distant switch is above the threshold level q_T or $\phi(t)$ is greater than the cell transmission rate $\phi_s(t)$. Otherwise, the allowed cell rate $\phi(t)$ should be increased.

In order to reduce the maximum queue length shown in Figure 5.3 (d) we replace the MS algorithm using Equations (5.4) and (5.5), which apply a use-it-or-lose-it policy to the three ABR sources. We can see from Figure 5.5 that the allowed cell rates at the moment of each burst arriving is lower than those in Figure 5.3 (a)-(c) and the maximum queue length is reduced from *13860* cells to *1628* cells, which implies a significant performance improvement.

In summary, the simulation results show that the stability of the MMS algorithm does not deteriorate in the presence of bursty sources. However, the stability of the MS algorithm does deteriorate. Although

the use-it-or-lose-it policy can be used to reduce the deterioration for the MS algorithm it should be pointed out that the maximum queue length is still much higher than that of the MMS algorithm. Moreover, the use-it-or-lose-it policy causes unfairness in the case where some sources adopt the policy and some do not adopt it.

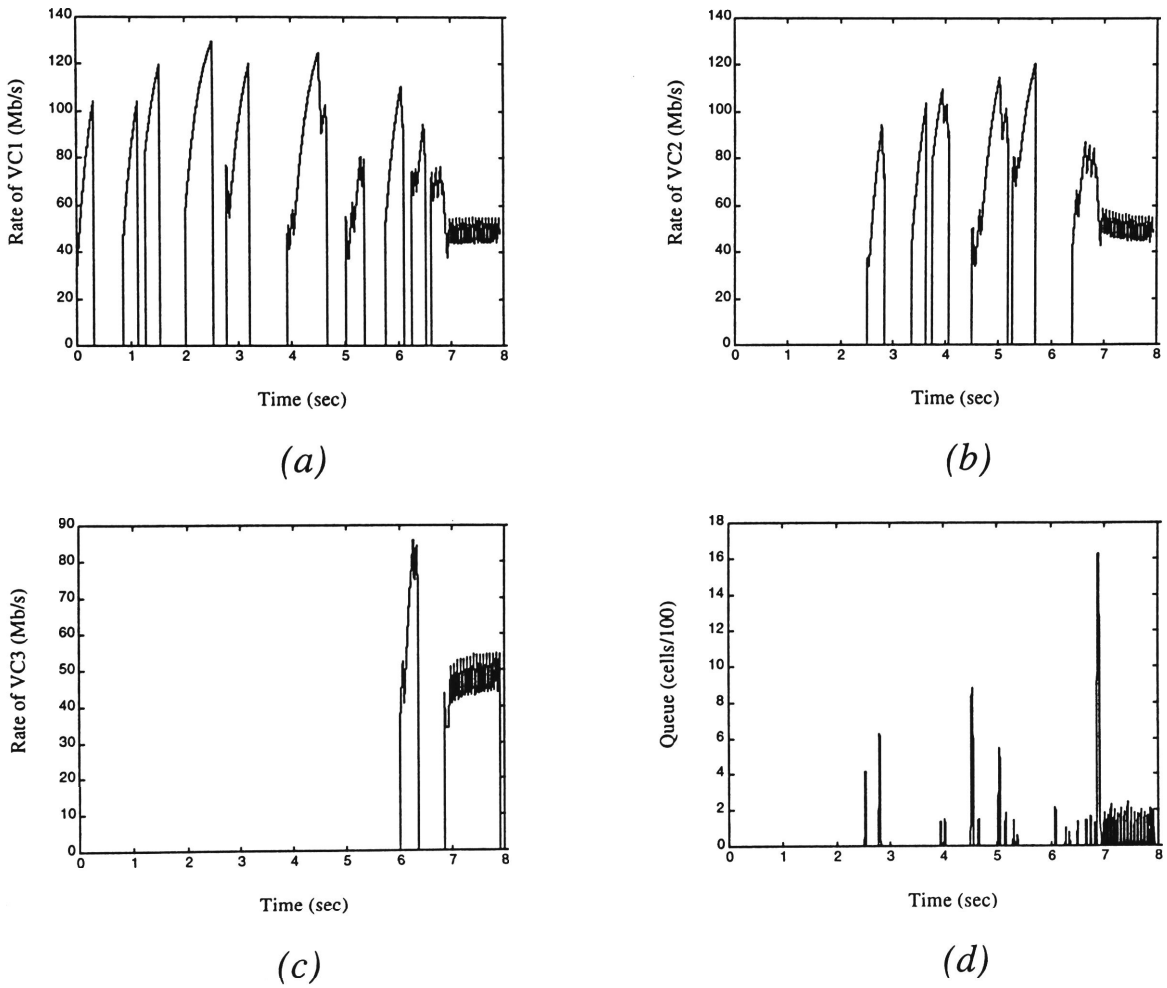

Figure 5.5 *Using use-it-or-lose-it policy. VC1, VC2 and VC3 turn on at 0, 2.5 s and 6 s. A=362 Mb/s^2, Γ=3.2 1/s, μ=155 Mb/s, τ_1=10 ms, τ_2=8 ms, τ_3=4 ms, $\nu_1=\nu_2=\nu_3$=34 Mb/s. Sources have the same intensity parameters as Figure 5.1, and adapted by the MS algorithm.*

5.3.2 Adding VBR/CBR background traffic

The examples considered so far assume that all the capacity is available for the ABR service. However, in practical networks there will also be CBR and VBR traffic sources which have higher priority than ABR traffic. In order to study the effects of the time-varying bandwidth on the performance of the binary feedback flow control system we add a CBR source and five VBR sources as background traffic.

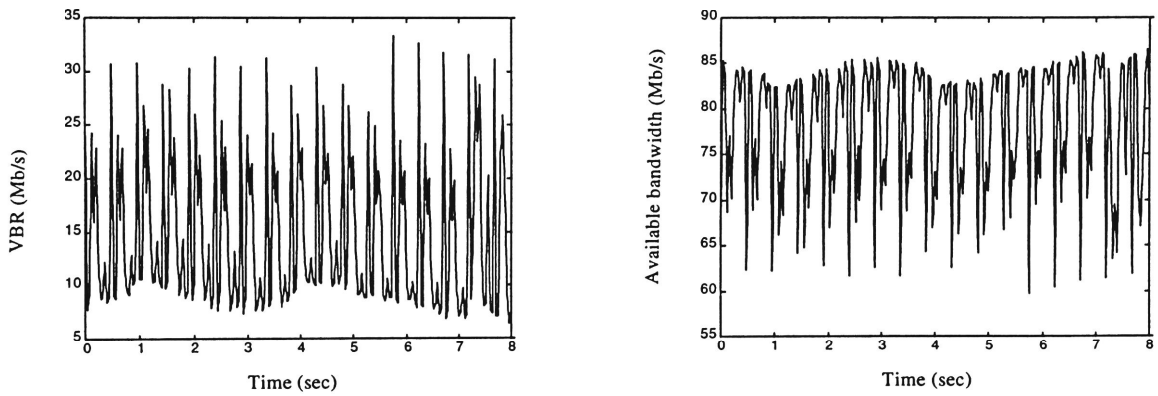

(a) *(b)*

Figure 5.6 *(a) The rate of VBR1+ VBR2+ VBR3+ VBR4+ VBR5. Mean arrival rate = 14.7 Mb/s.*
(b) The available bandwidth for ABR sources.

The CBR source has an arrival rate of *62 Mb/s* which is *40%* of the link capacity. As shown in Figure 5.6 (a) we choose five MPEG (ISO Moving Picture Expert Group) video encoded sequences as VBR traffic. In the network there are six bursty ABR sources having the intensity parameters $\lambda_1=3$ and $\lambda_2=500$. They are turned on at the times *0, 0.5 s, 1 s, 1.5 s, 2 s, 2.5 s*. The available bandwidth for ABR sources can be calculated using *μ-CBR-VBR* as shown in Figure 5.6 (b). Parameters of MMS algorithm

are determined according to Equation (4.11). Which implies that the target bandwidth for ABR sources is $k\mu$. Depending on k it may be higher than the available bandwidth μ-*CBR-VBR*. As a result, congestion can occur in both transient and steady states. It should be pointed out that if CBR and the mean value of the VBR traffic rate is available it can be used to determine parameters of the MMS algorithm by modifying Equation (4.11) in a similar fashion in order to improve the performance of the network. However, the information about CBR and the mean rate of VBR traffic is usually unavailable for ABR sources.

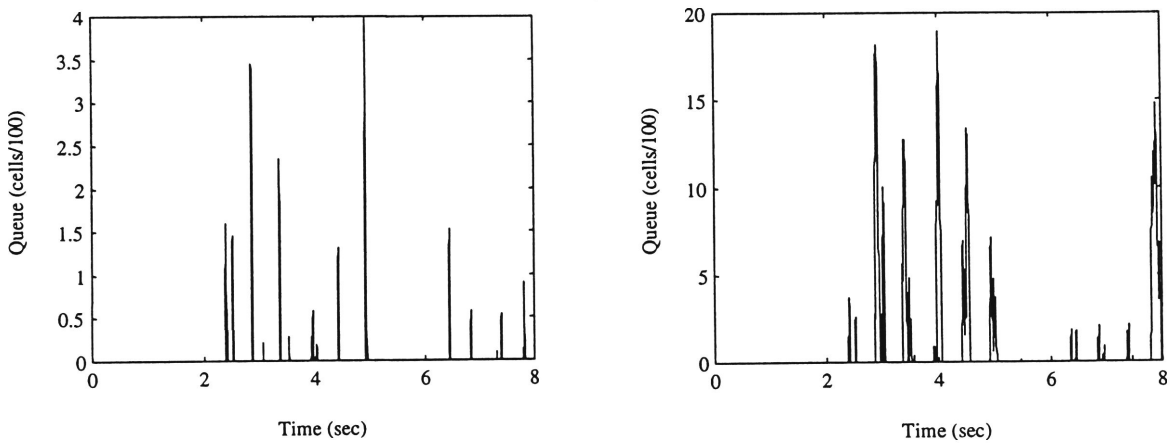

(a) *(b)*

Figure 5.7 *The performance of MMS and MS algorithms under CBR/VBR background traffic.* Γ*=3.2 1/s,* μ*=155 Mb/s,* τ_1*=2 ms,* τ_2*=4 ms,* τ_3*=6 ms,* τ_4*=8 ms,* τ_5*=10 ms,* τ_6*=2 ms,* ν_i*=3 Mb/s for* $i=1,2,\ldots,6$*. Sources have intensity parameters* λ_1*=3,* λ_2*=500 and a packet =80 cells, k=0.95, and use-it-or-lose-it policy is applied.*

(a) MMS: $A^+(t)$*=462 Mb/s*^{2} *for J=1,* $A^+(t)$ *=226 Mb/s*^{2} *for J=2,* $A^+(t)$*=147 Mb/s*^{2} *for J=3,* $A^+(t)$*=108 Mb/s*^{2} *for J=4,* $A^+(t)$*=85 Mb/s*^{2} *for J=5,* $A^+(t)$*=69 Mb/s*^{2} *for J=6,* $A^- \equiv 462$ *Mb/s*^{2}.

(b) MS: $A=462$ *Mb/s*^{2}.

The result of MMS algorithm is shown in Figure 5.7 (a). As predicted the queue in the distant switch builds up frequently during entire observation period. The designed target bandwidth $k\mu$ is chosen to be 147 Mb/s considering the assumption that the bandwidth requirement for CBR and VBR is unknown in ABR sources. Certainly, it is higher than the available bandwidth for ABR sources as shown in Figure 5.6 (b). The maximum queue length is *398* cells.

Simulation for ABR sources using the MS algorithm is carried out for comparison. Figure 5.7 (b) shows that the MS algorithm leads to more frequent and more intense congestive periods. As a result the maximum queue length reaches to *1894* cells, which is much higher than that produced by the MMS algorithm shown in Figure 5.7 (a).

5.4 Conclusion

We have studied the performance of the binary feedback flow control mechanisms under the bursty ABR sources and the VBR/CBR background traffic using simulation. In the case where all the link capacity is available for ABR sources, the MS algorithm leads to longer queue lengths which result in longer delays. The queue can be reduced by using a simple use-it-or-lose-it policy at the cost of unfairness. By comparison, the MMS algorithm causes no oscillation in the network and, hence, no queuing delay. In the case of time-varying available bandwidth for ABR sources, the MMS algorithm minimises congestion duration and intensity significantly.

Chapter 6

Conclusion and Further Research Issues

6.1 Conclusion

Congestion control is an important issue for efficient traffic management in ATM networks. The ATM Forum has defined the available bit rate (ABR) service which is designed to share the available bandwidth among all active ABR users. The ABR service attempts to minimise cell loss while sharing fairly across ABR connections. This is a difficult task because of delayed feedback information and time-varying available bandwidth associated with the ABR services. This thesis investigates the performance of the MS algorithm and proposes a design procedure for ABR flow control schemes.

We consider the same network structure as used by Bonomi, Mitra and Seery (1995), where a number of greedy sources are trying to send cells to a distant switch buffer and the sources adapt their rates using the MS algorithm. In Chapter 2, we derived an analytical model of the switched network together with the MS algorithm in Laplace domain and described it in block diagram form using transfer functions and nonlinear elements. The model clearly shows the feedback structure, which can help us better understand the binary feedback flow control system. Furthermore, the derived model can be easily extended from the single VC case to the multiple VCs.

In Chapter 3, we investigated the stability and sustained oscillation in the binary feedback system. Frequency and amplitude of the limit cycle are obtained using an approximate frequency domain technique known as Describing Function. The results shown that sustained oscillation exists during the steady state when $\frac{A}{\Gamma J}(\mu - \sum_{i=1}^{J} \nu_i) < 1$. The higher the gain A, the greater the oscillation amplitude. The amplitude of queue oscillation

will also increase as the number of active VCs increases or the damping Γ decreases. Moreover, an increase in the average time delay of the active VCs will also cause an increase in the amplitude and a decrease in the frequency of oscillation. The accuracy of the DF approach is investigated by harmonic analysis. The results indicate that the DF approach is effective when the ratio of Γ/A is low. However, the accuracy deteriorates as the ratio approaches $1/(\mu-\nu)$. In the later case the oscillating waveform differs greatly from the assumed sinusoidal function thus violating the underlying assumption of the DF approach.

Analytic results reveal the relationship between the optimal operating point and basic parameters such as gain, damping and the number of active VCs. They provide useful guidelines for minimising the oscillation behaviour of the MS algorithm. In Chapter 4, a modified MS algorithm is proposed using time-varying gain instead of constant gain in order to maintain the near optimal operating point. Simulation results show the MMS algorithm results in an oscillation-free system while maintaining fairness across ABR connections during the steady state. Simulation tests were also carried out to demonstrate the affects of the rate decrease gain A^- and the minimum cell rate ν. The results shown that a higher gain A^- can be used for minimising congestion intensity during the transient state and a lower starting rate also leads to much smaller queue lengths during the transient state.

In Chapter 5, the performance of the MMS algorithm was demonstrated and compared with the MS algorithm under a more realistic network environment, where bursty rather than greedy sources are used for ABR traffic. We also examine the affects of VBR/CBR background traffic sources. Simulation results show that the MMS algorithm is still fair and

oscillation-free for the case where ABR sources represent the entire traffic on the link. Large queue lengths arise when ABR sources are subjected to the MS algorithm. This queue length can be reduced by implementing a simple use-it-or-lose-it policy at each ABR source at the cost of unfairness. When VBR/CBR traffic is added, the MMS algorithm produces a much smaller queue length than the MS algorithm.

6.2 Further research issues

The following research issues open for further investigation.

6.2.1 Buffer nonlinearity

The analysis presented in Chapter 3 only applies for a nonempty buffer or empty buffer where the input rate in the buffer is higher than or equal to its service rate. Under this assumption, Equation (2.1) is simplified into the linear equation

$$\frac{d}{dt}q(t) = \phi(t - \tau / 2) - \mu \qquad (6.1)$$

However, when the buffer threshold level q_T is set very low, the linear buffer assumption does not apply. Further research is required to study the possibility for the DF analysis to be applied to the situation where the buffer has nonlinearity. Such an analysis may lead to the relationship between the oscillation behavior and the controller parameters under more realistic condition and will be useful in designing new binary flow control schemes.

6.2.2 Analysis of transient state

The analysis of the sustained rate oscillations was undertaken in Chapter 3. As a result, the MMS algorithm was proposed in order to eliminate limit cycle behaviour. In the MMS algorithm the parameter ratio A^{-}/Γ^{-} is used to decreases the allowed cell rate during congestion after adding new VCs. The simulation results indicated that a larger ratio of A^{-}/Γ^{-} is of benefit to reduce the maximum queue length. However, the optimal A^{-}/Γ^{-} has not been determined. Transient state analysis is required in order to select the optimal A^{-}/Γ^{-} rate.

6.2.3 Estimating the number of active VCs

The MMS algorithm proposed in Chapter 4 uses the optimal parameter A/Γ ratio to achieve oscillation-free operation, fair implementation and high link utilisation during steady state. As an additional condition, the information about the active VC number J is required by the sources. Further research needs to be carried out on estimating the number of active VCs from the system behaviour under more realistic situations in which J is unknown at the sources.

Author's Publications and References

Chicharo, J.F., Xue, L. and Eyers, T., (1998) "On the design of a binary feedback flow control algorithm with limit cycle-free behaviour", APCC'98, vol. 3, pp. 1561-1565.

Xue, L., Chicharo, J.F. and Li, Z., (1996) "Analysis/simulation of the MS adaptive algorithm for feedback flow control in high speed wide-area networks", Australian Telecommunication Networks and Application Conference, Melbourne, pp. 543-548.

Afek, Y., Mansour, Y. and Ostfeld, Z., (1996) "Phantom: a simple and effective flow control scheme", ACM SIGCOMM'96, pp.169-182.

Atherton, D. P., (1981) "Stability of nonlinear systems", Research Studies Press.

ATM Forum Technical Committee, (1996) "Traffic Management specification", Version 4.0, ATM forum 195-0013R10.

Barnhart, A., (1994) "Baseline performance using PRCA rate-control", ATM Forum/94-0597.

Barnhart, A., (1994) "Use of the extended PRCA with various switch mechanisms", ATM Forum/94-0898.

Barnhart, A., (1994) "Explicit rate performance evaluation", AF-TM 94-0983R1.

Bennett, J. and Jardins, T. D., (1994) "Comments on the July PRCA rate-control baseline", ATM Forum/94-0682.

Bolot, J. C. and Shankar, A. U., (1990) "Dynamical behaviour of rate-based flow control Mechanisms", Computer and Communication Review, vol. 30, pp. 35-49.

Bonomi, F. and Fendick, K., (1995) "The rate-based flow control framework for the available bit rate ATM service," IEEE Network, vol. 9, no. 2, pp. 25-39.

Bonomi, F., Mitra, D. and Seery, J. B., (1995) "Adaptive algorithms for feedback-based flow control in high-speed, wide-area ATM networks", IEEE Journal on Selected Areas in Communications, Vol. 13, pp. 1267-1283.

Charney, A., Clark, D. D. and Jain, R., (1995) "Congestion Control with Explicit Rate Indication," IEEE ICC'95, pp. 1954-1963.

Chen, T. M., Liu, S. S. and Samalam, V. K., (1996) "The available bit rate service for data in ATM networks", IEEE Communication Magazine, May, pp. 56-71.

Chiussi, F. M., Xia, Y. and Kumar, V. P., (1996) "Dynamic max rate control algorithm for available bit rate service in ATM networks", IEEE GLOBECOM'96, pp. 2108-2117.

Fendick, K. W., Rodrigues, M. A. and Weiss, A., (1992) "Analysis of a rate-based feedback control strategy for long haul data transport", Performance Evaluation, vol. 16, pp. 67-84.

Gelb, A. and Velde, W. E. V., (1968) "Multiple-Input Describing Functions and Nonlinear System Design", Mcgraw-Hill Book Company.

Hluchyj, M. and Yin, N., (1994) "On close-loop rate control for ATM networks", INFOCOM'94, pp. 99-108.

Hughes, D., (1994) "Fairness share in the context of MCR", ATM Forum Contribution/94-0977.

Jacobson, V., (1988) "Congestion avoidance and control", ACM SIGCOMM'88, pp.314-329.

Jain, R., (1996) "Congestion control and traffic management in ATM networks: recent advances and a survey," Computer Networks and ISDN Systems, Vol. 28, pp. 1723-1738.

Jain, R. *et al.*, (1995) "Bursty ABR sources", ATM Forum/95-1345.

Jain, R. *et al.*, (1996) "Comments on 'use-it or lose-it'", ATM Forum/96-0178.

Jain, R., Kalyanaraman, S. and Viswanathan, R., (1994) "The OSU scheme for congestion avoidance using explicit rate indication", AF-TM 94-0883.

Jain, R., Kalyanaraman, S. and Viswanathan, R., (1994) "The EPRCA+ scheme", AF-TM 94-0988.

Jain, R., Kalyanaraman, S. and Viswanathan, R., (1995) "A simple switch algorithm", AF-TM 95-0178R1.

Jain, R., Ramakrishnan, K. K. and Chiu, D., (1988) "Congestion avoidance in computer networks with a connectionless network layer", Technical Report DEC-TR-506, Digital Equipment Corporation.

Krishnan, R., (1997), "Rate-based control schemes for ABR traffic - design principles and performance comparison", Computer Networks and ISDN Systems, vol. 29, pp. 583-593.

Kolarov, A. and Ramamurthy, G., (1996) "Comparison of explicit rate and explicit forward congestion indication flow control schemes for ABR service", IZS'96.

Kung, H., Blackwell, T. and Chapman, A.., (1994) "Credit-based flow control for ATM networks: credit update protocol, adaptive credit allocation, and statistical multiplexing", SIGCOMM'94, pp. 101-114.

Kung, H. and Morris, R., (1995) "credit-based flow control for ATM network", IEEE Network, Vol. 9, pp. 40-48.

Li, S. Q. and Hwang, C., (1993) "Queue response to input correlation function: continuous spectral analysis", IEEE/ACM Trans. Networking, vol. 1, pp. 678-692.

Liu, T., Anido, G. and Chicharo, J., (1995) "Local area network traffic charactersation and modeling", ATNAC'95, pp. 335-339.

Math Works Inc., (1996) "The Student Edition of SIMULINK", Prentice Hall, Englewood Cliffs, NJ.

Michelle, R. M., (1996) "ABR: smart bandwidth", ATM ABR Standard-Lan Time, 601b001b.html.

Mitra, D., (1988) "stochastic theory of a fluid model of producers and consumers coupled by a buffer", Adv. Appl. Prob. Vol. 20, pp. 646-676.

Mitra, D. and Seery, J. B., (1993) "New dynamic adaptive algorithms for windows and rates in high speed wide area networks based on periodic, 1-bit, explicit feedback", unpub. Report.

Mukherjee, A. and Strikwerda, J. C., (1991) "Analysis of dynamic congestion control protocols-A Fokker-planck approximation," ACM SIGCOMM'91, pp.159-169.

Newman, P., (1994) "Traffic management for ATM local area networks", IEEE Communication Magazine, vol. 32, pp. 44-50.

Ogata, K., (1990) "Model Control Engineering", Second edition, Prentice Hall, Englewood Cliffs, NJ.

Ohsaki, H., Murata, M., Suzuki, H., Ikeda, C. and Miyahara, H., (1995) "Analysis of rate-based congestion control algorithms for ATM networks - part 1: steady state analysis", GLOBECOM'95, pp. 296-303.

Pitts, J. M. and Schormans, J. A., (1996) "Introduction to ATM design and performance: with application analysis software", John Wiley & Son.

Rammamurthy, G. and Ren, Q., (1995) "analysis of the adaptive rate control for ABR service in ATM networks", GLOBECOM'95, pp. 1083-1088.

Ramakrishnan, K. K., Chiu, D. M. and Jain, R., (1987) "Congestion avoidance in computer networks with a connectionless network lay. Part IV: a selective binary feedback scheme for general topologies," Digital Equipment Corporation, Technical Report DEC-TR-510.

Ramakrishnan, K. K. and Jain, R., (1988) "A binary feedback scheme for congestion avoidance in computer networks with a connectionless network layer", ACM SIGCOMM'88, pp. 303-313.

Ramakrishnan, K. K. and Mitra, D., (1988) "PANACEA : An integrated set of tools for performance analysis", Modeling Techniques and Tools for Computer Evaluations, R. Puigjaner and D. Potier, Eds. New York Plenum, 1988, pp. 25-40.

Roberts, L., (1994) "Enhanced PRAC (proportional rate-control algorithm)", ATM Forum/94-0735R1.

Roberts, L. *et al.*, (1994) "Closed-loop rate-based traffic management", ATM Forum Contribution 94-0438R1.

Roberts, L. *et al.*, (1994) "New pseudocode for explicit rate plus EFCI support", ATM Forum/94-0974.

Sathaye, S., (1994) "ATM Forum traffic management specification", ATM Forum Contribution.

Siu, K-Y. and Tzeng, H-Y., (1995) "Intelligent congestion control for ABR service in ATM networks", Computer Communication Review, Vol. 24, pp. 81-105.

Stallinys, W., (1997) "Data and computer communications", Prentice Hall, London.

West, J. C., (1960) "Analytical techniques for non-linear control systems", The English Universities Press LTD, London.

Yang, C. and Reddy, A. V. S., (1995) "A taxonomy for congestion control algorithms in packet switching networks", IEEE Network, vol. 11, July/August, pp. 34-45.

Yin, N., (1994) "Fairness definition in ABR service model", ATM Forum Contribution/94-0928R2.

Yin, N., (1995) "Analysis of a rate-based traffic management mechanism for ABR service", GLOBECOM'95, pp. 1076-1082.

Zhao, Y., Li, S. Q. and Sigarto, S., (1996) "A linear dynamic model for design of stable explicit-rate ABR control schemes", ATM Forum /96-0606.

Appendix A *Results - Bonomi, Mitra and Seery (1995)*

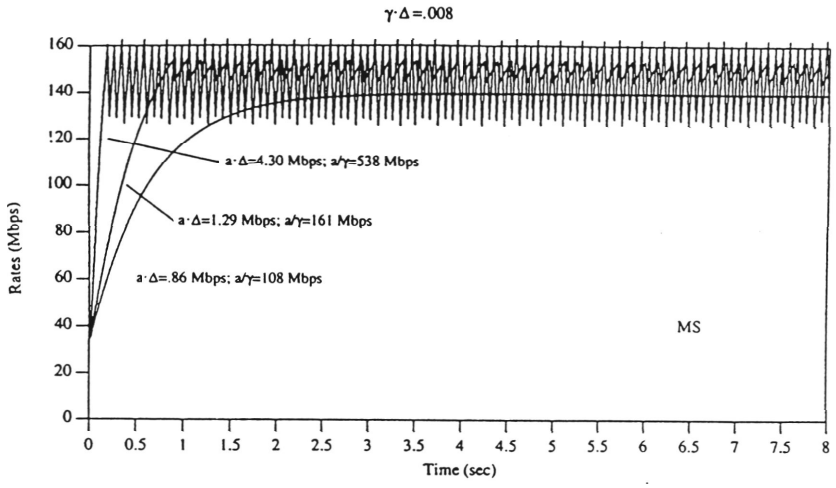

Fig. 4. Various values of ratio a/γ for one VC. μ = 155 Mb/s, ν = 34 Mb/s, τ = 10 ms, Δ = 5 ms, σ = 1.0, and Q_T = 6.5 cells. MS algorithm.

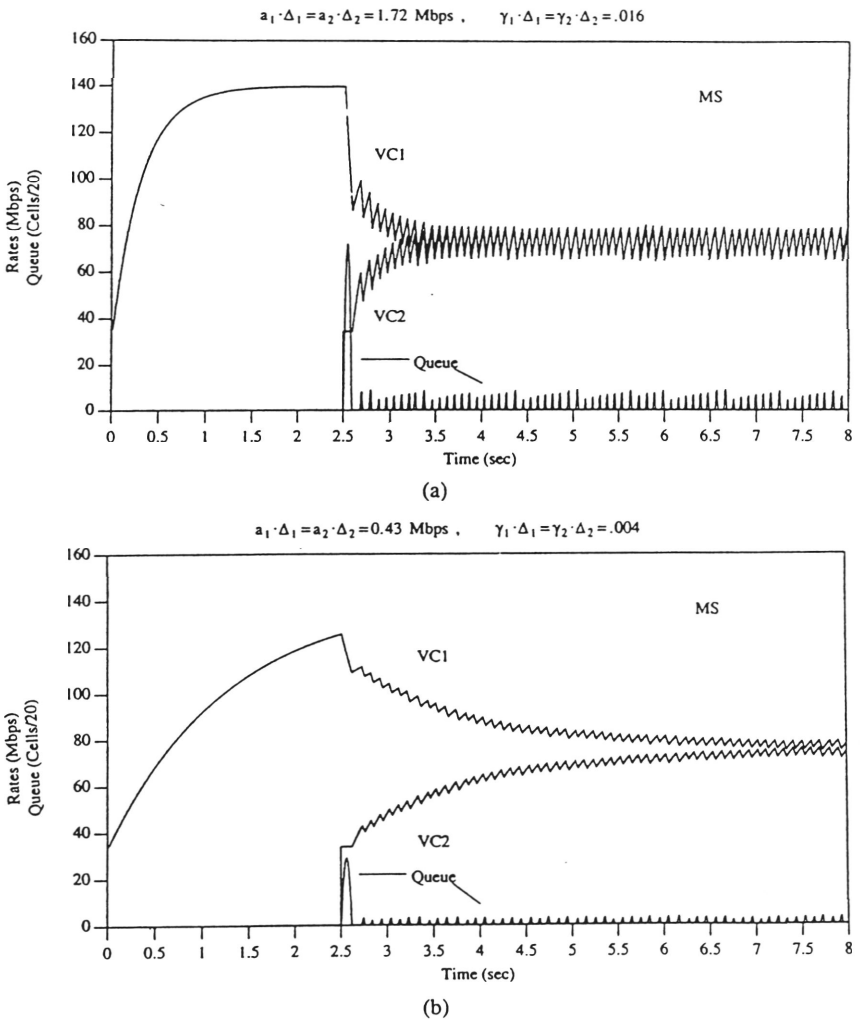

Fig. 5. Various gains and damping constants with ratio a/γ held fixed at 108 Mb/s and ν = 34 Mb/s. VC1 turns on at time 0 and VC2 at 2.5 s. μ = 155 Mb/s, τ_j = 10 ms, Δ_j = 5 ms, σ_j = 1.0, (j = 1, 2), and Q_T = 6.5 cells. MS algorithm.

Appendix B *Proof for the amplitude of oscillation increasing as the number of active VCs increase*

Proof: Let ω_1 denotes the frequency of limit cycle for a single VC and $\omega_{\Sigma J}$ for multiple VCs, D_1 represent amplitude of queue oscillation for a single VC and $D_{\Sigma J}$ for multiple VCs. Letting

$$\tau_1 + \tau_2 + \ldots + \tau_J = \beta\tau_1 \quad (\beta > 1) \tag{B-1}$$

From (3.16), (3.24) and (B-1) we have

$$\omega_{\Sigma J} \approx \sqrt{\Gamma \Big/ \left(\frac{1}{J}\sum_{i=1}^{J}\tau_i\right)} = \sqrt{\frac{J\Gamma}{\beta\tau_1}} = \sqrt{\frac{J}{\beta}}\omega_1 \tag{B-2}$$

substituting (B-2) into (3.23) it follows

$$D_{\Sigma J} \approx \frac{4AJ}{\pi\omega_{\Sigma J}\sqrt{\omega_{\Sigma J}^2 + \Gamma^2}}\cos\left[\frac{\pi\Gamma}{2AJ}\left(\mu - \sum_{i=1}^{J}\nu_i\right)\right]$$

$$\approx \frac{4AJ}{\pi\sqrt{\frac{J}{\beta}}\omega_1\sqrt{\frac{J}{\beta}\omega_1^2 + \Gamma^2}}\cos\left[\frac{\pi\Gamma}{2AJ}\left(\mu - \sum_{i=1}^{J}\nu_i\right)\right]$$

$$\approx \frac{4A}{\pi\omega_1\sqrt{\frac{\omega_1^2}{\beta^2} + \frac{\Gamma^2}{J\beta}}}\cos\left[\frac{\pi\Gamma}{2AJ}\left(\mu - \sum_{i=1}^{J}\nu_i\right)\right] \tag{B-3}$$

When the number of active VCs increases to J+1 we let

$$\tau_1 + \tau_2 + \ldots + \tau_J + \tau_{J+1} = h\tau_1 \tag{B-4}$$

and know from (B-1) and (B-4) that $h > \beta > 1$.

Replacing J and β Using J+1 and h in (B-3), we have

$$D_{\Sigma J+1} \approx \frac{4A}{\pi\omega_1\sqrt{\frac{\omega_1^2}{h^2}+\frac{\Gamma^2}{(J+1)h}}}\cos[\frac{\pi\Gamma}{2A(J+1)}(\mu-\sum_{i=1}^{J+1}v_i)] \qquad \text{(B-5)}$$

Noting that J is the number of active VCs which is a positive integer, it follows that

$$\cos[\frac{\pi\Gamma}{2A(J+1)}(\mu-\sum_{i=1}^{J+1}v_i)] > \cos[\frac{\pi\Gamma}{2AJ}(\mu-\sum_{i=1}^{J}v_i)] \qquad \text{(B-6)}$$

Because of $h > \beta > 1$ we have

$$\frac{\omega_1^2}{h^2}+\frac{\Gamma^2}{(J+1)h} < \frac{\omega_1^2}{\beta^2}+\frac{\Gamma^2}{J\beta} \qquad \text{for J>1, β>1, h>1.} \qquad \text{(B-7)}$$

Substituting (B-6) and (B-7) into (B-5), we know

$$D_{\Sigma J+1} > \frac{4A}{\pi\omega_1\sqrt{\frac{\omega_1^2}{\beta^2}+\frac{\Gamma^2}{J\beta}}}\cos[\frac{\pi\Gamma}{2AJ}(\mu-\sum_{i=1}^{J}v_i)] \qquad \text{(B-8)}$$

The right side of (B-8) equals to (B-3), which implies

$$D_{\Sigma J+1} > D_{\Sigma J} \qquad \text{(B-9)}$$